

***De novo* fragment-based design of inhibitors of DXS guided by  
spin-diffusion-based NMR spectroscopy**

T. Masini, J. Pilger, B. S. Kroezen, B. Illarionov, P. Lottmann, M. Fischer\*, C. Griesinger\*,  
A. K. H. Hirsch\*

## Table of contents

Figures (Figures S1–S16)	S3
Tables (Table S1)	S16
Schemes (Scheme S1–S6)	S17
Modelling and docking	S20
Construction of Expression Vector pET22b-H6TBKDRDXS	S21
Purification of DXS from <i>D. radiodurans</i> and <i>M. tuberculosis</i>	S21
Photometric assay for kinetic studies of DXS	S22
Calculation of $K_i$ values	S23
Experimental procedure for NMR analysis	S24
Procedures for the MD simulations	S24
Experimental procedures	S25
NMR spectra	S42
References	S56

```

          10          20          30          40          50          60
          |          |          |          |          |          |
DXS_MYCTUB -----MLQQIRGPADLQHLSQLRELAAEIREFLIHKVAATGGHLGPNLGVVE
DXS_DEIRAD MNELPGTSDTPLLQIHGPKDLKRLSREQLPALTEELRGEIVRVCSRGGHLHLASSLGAVD
TK_HOMSAP  -MESYHKPDQQKLQALKDTANLRIS--SIQASSAAGSG--HPTSCCSAAVIMAVLFFHT
          * : : : : : : * : : : : : : . . : . *

          70          80          90          100         110         120
          |          |          |          |          |          |
DXS_MYCTUB LTLALHRVFDSPHDFPIIFDTGHQAYVHKMLTGRS-----QDFATLRKKGGLSGYPSRAES
DXS_DEIRAD IITALHYVLDSPRDRILFDVGHQAYAHKILTGRR-----DQMADIKKEGGISGFTKVSES
TK_HOMSAP  MRYKSQDPRNPHNDRFVLSKGHAAPILYAVWAEAGFLAEAE LLNLRKISSDLDGHPVPKQ
          : : : . * : : : * * : : : : : : : : * : : . . . : :

          130         140         150         160         170         180
          |          |          |          |          |          |
DXS_MYCTUB EHDWVESHASAAALSYADGLAKAFELTGHRNRHVAVVGDGALTGGMCWEALN NIAASRR
DXS_DEIRAD EHDAITVGHASTSLANALGMALARDAQGK-DFHVAAVIGDGLTGGMALAALNTIGDMGR
TK_HOMSAP  AFTDVATGSLGQGLGAACGMAYTGKYFDKASYRVYCLLDGDELSEGSVWEAMAFASIYKL
          . : . . * . * * : . . : . * : : * * * * : * : * : .

          190         200         210         220         230         240
          |          |          |          |          |          |
DXS_MYCTUB PVIIVVNDNGRSYAPTIGGVADHLATLRLQPAYEQALETGRDLVRAVPLVGGWLWFRFLHS
DXS_DEIRAD KMLIVLNDNEMSI SENVGAMNKEMRGLQVQKWFQEGEGAGKKA VEAVSKP---LADFMSR
TK_HOMSAP  DNLVAILDINR-----LGQSDPAPLQHQM DIYQKRCEAFGWHA IVDGHS----VEELCK
          : : : * : * : : : : : : * . : . : : :

          250         260         270         280         290         300
          |          |          |          |          |          |
DXS_MYCTUB VKAGIKDSLSPQLL--FTDLGLKYVGPVDGHD ERAVEVALRSARRFGAPVIVHVTRKGM
DXS_DEIRAD AKNSTRHFFDPASVNPFAAMGVRYVGPVDGHN VQELVWLLERLVDLDGPTILHIVTTK GK
TK_HOMSAP  AFGQAKHQPTAI IAKTFKGRGITGVEDKESWHGKPLP---KNMAEQIIQEIYSQIQSKKK
          . : . . * * : * : : : : . * : *

          310         320         330         340         350         360
          |          |          |          |          |          |
DXS_MYCTUB GYPPAEADQAEQMHSTVPI DPATGQATKVAGPGWTATFSDALIGYAQKRRDIVAITAAMP
DXS_DEIRAD GLSYAEADP-IYWHGPAKFD PATGEYVPSAYSWSAAFGEAVTEWAKTDPRTFVVT PAMR
TK_HOMSAP  ILATPPQEDAPSVDIANIRMPSPSYKVGDKIATR KAYGQALAKLGHASDR IIALDGDTK
          . . : . . * : . . . : : : * : : : : :

          370         380         390         400         410         420
          |          |          |          |          |          |
DXS_MYCTUB GPTGLTAFGQRFDPDR LFDVGI AEQHAMTSAAGLAMGG-LHPVVAIYSTFLNRAFDQIMMD
DXS_DEIRAD EGSGLVEF SRVHPHRYLDVGI AEEVAVTTAAGMALQG-MRPVVAIYSTFLQRAYDQVLHD
TK_HOMSAP  NSTFSEIFKKEHPDRFIECYIAEQNMVSI AVGCATRNRTPFCSTFAAFFTRA FDQIRMA
          : * : . * * : : * * : : * * * . * : : : * * : * * :

          430         440         450         460         470         480
          |          |          |          |          |          |
DXS_MYCTUB VALHKL PVTMVLDRAGITGSDGASHNGMWDLSMLGIVPGIRVAAPRDATRLREELGEALD
DXS_DEIRAD VAIEHLNVTFCIDRAGIVGADGATHNGVFDLSFLRSIPGVRI GLPKDAAELRGML-KYAQ
TK_HOMSAP  AISESNINLCGSHCGVSI GEDGASQMALEDLAMFRSVPTSTVFYPSDGVATEKAV-ELAA
          . . . . * * * : : * * : : * : * * . . : :

          490         500         510         520         530         540
          |          |          |          |          |          |
DXS_MYCTUB VDDGPTALRFPKGDVGEDISALERRGGVDVLAAPADGLN--HDVLLVAIGAFAPMALAVA

```

```

DXS_DEIRAD   THDGPFAIRYPRGNT---AQVPAG-TWPDLKWGEWERLKGDDVVILAGGKALDYALKAA
TK_HOMSAP    NTKGICFIRTSRPEN---AIIYNNNEDFQVGQAKVVVLKSKDDQVTVIGAVTLHEALAAA
              .*  :*  .:  :                ::  .      .  .:*  :.:  *      **  .*

              550      560      570      580      590      600
              |        |        |        |        |        |
DXS_MYCTUB   KRLHNQGIGVTVIDPRWVLPVSDG-VRELAVQHK-LLVTLEDNGVNGGAGSAVSAALRRA
DXS_DEIRAD   EDLP----GVGVVNARFVKPLDEEMLREVGGRRAR-ALITVEDNTVVGGFGGAVLEALNSM
TK_HOMSAP    ELLKKEKINIRVLDPFTIKPLDRKLIILDSARATKGRILTVEDHYEYEGGIGEAVSSAVVG-
              :  *      .:  *:..  :  *:.  :  :  .  :  :  :  :  :  :  :  :  :  :  :
              610      620      630      640      650      660
              |        |        |        |        |        |
DXS_MYCTUB   EIDVPCRDRVGLPQEFYEHASRSEVLADLGLTDQDVARRITGWVAALGTGVCASDAIPEHL
DXS_DEIRAD   NLHPTVRVLGIPDEFQEHATAESVHARAGID----APAIRTVLAEELGVDVPIEV-----
TK_HOMSAP    EPGITVTHLAVN-RVPRSGKPAELLKMFGIDRDAIAQAVRGLITKA-----
              :  .      .:  :  .  .  .  .  :  *  :  *  :  :  :

DXS_MYCTUB   D
DXS_DEIRAD   -
TK_HOMSAP    -

```

**Figure S1.** Alignments of *Mycobacterium tuberculosis* DXS (upper sequence, acc. no. YP\_177898, 638 residues), *Deinococcus radiodurans* DXS (acc. no. Q9RUB5, 629 residues) and human transketolase (bottom sequence, acc. No. CAA47919, 623 residues). Dashed lines indicate gaps introduced in protein sequences in order to maximise the alignment. Asterisks indicate amino-acid residues (AARs) that are identical between two protein sequences, colons indicate AARs that are strongly similar and points indicate AARs that are weakly similar between the three protein sequences. The alignment has been performed using the online CLUSTAL W (1.8) multiple sequence alignment server ([http://npsa-pbil.ibcp.fr/cgi-bin/npsa\\_automat.pl?page=/NPSA/npsa\\_clustalw.html](http://npsa-pbil.ibcp.fr/cgi-bin/npsa_automat.pl?page=/NPSA/npsa_clustalw.html)). The following parameter could be extracted from the alignment: Identity (\*): 74 is 11.20%, Strongly similar (:): 108 is 16.34%, Weakly similar (.): 78 is 11.80%, Different: 401 is 60.67%.

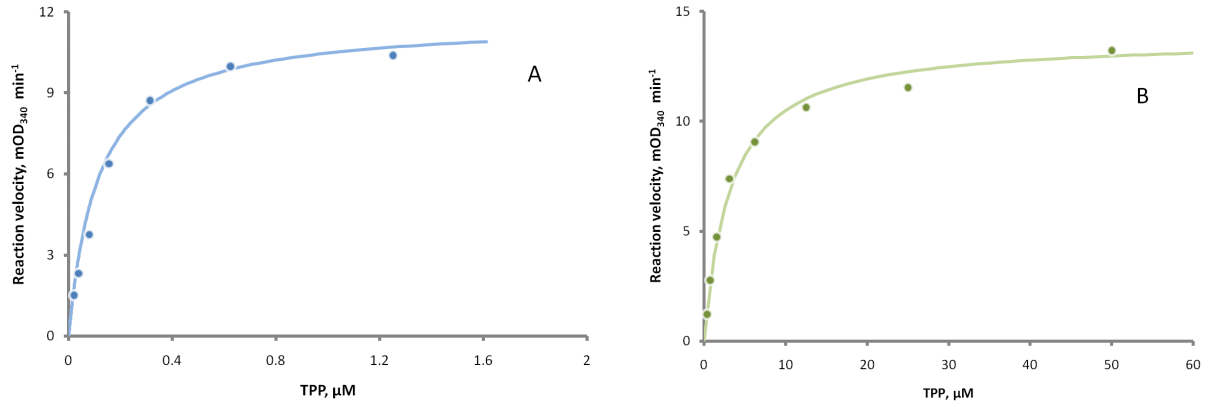


**Figure S2.** Reaction velocity *versus* thiamine diphosphate (TDP) concentration plots for *D. radiodurans* DXS (A) or *M. tuberculosis* DXS (B).

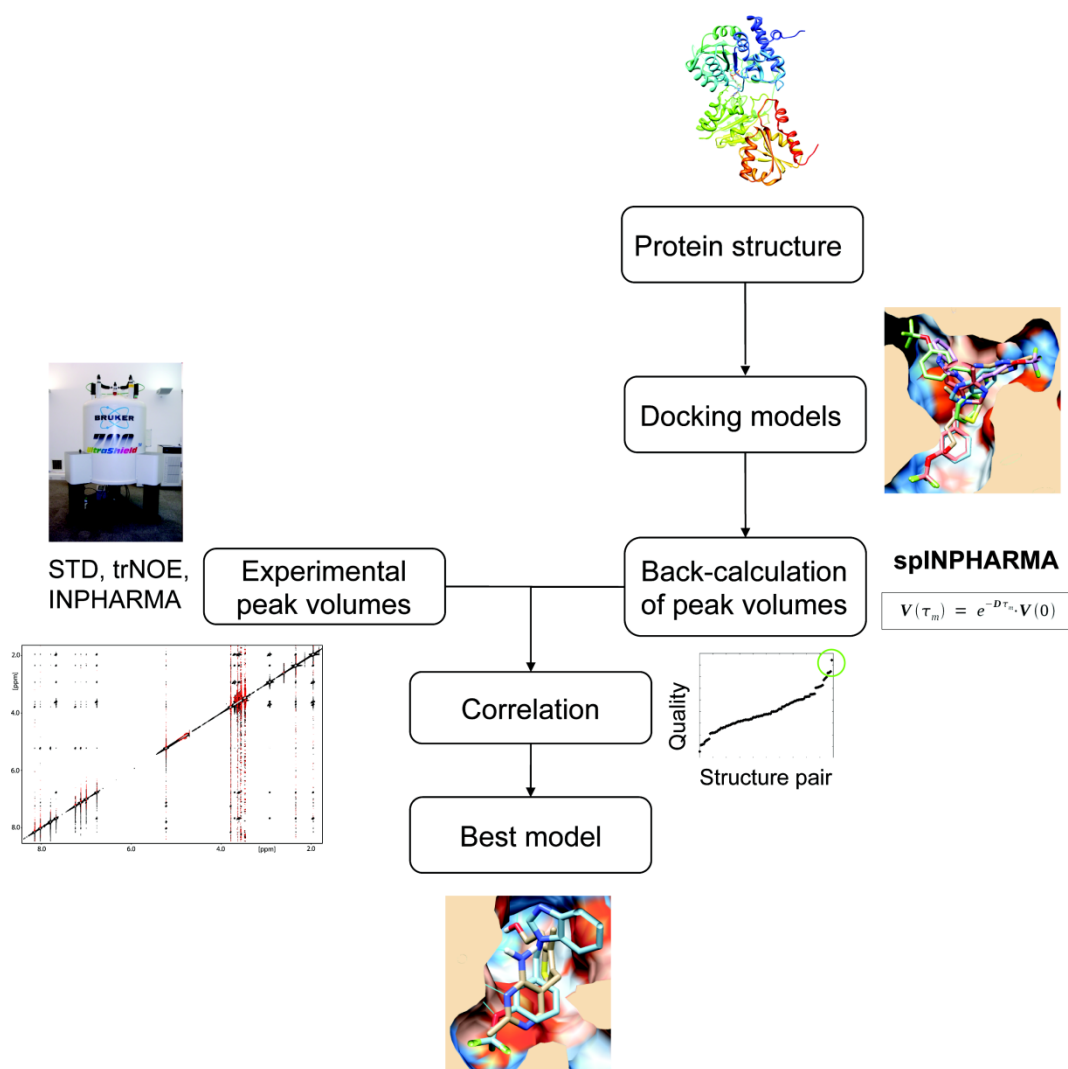


**Figure S3.** Flowchart to illustrate the binding-mode validation by spin-diffusion-based NMR spectroscopy. In the first stage, the protein structure of DXS (PDB code: 2O1X)<sup>[1]</sup> was taken, and docking models of the ligands were created within the TDP-binding site using the docking software FlexX.<sup>[2]</sup> Representative docking poses with acceptable torsion energies were chosen and the spin-diffusion-based NMR parameters STD, trNOE and INPHARMA were back-calculated with the software spINPHARMA ([www.inpharma.de](http://www.inpharma.de)). These parameters were also experimentally determined and correlated with the back-calculated values. The docking pose with the best correlation between experimental and back-calculated values was then taken as the experimentally validated binding mode.

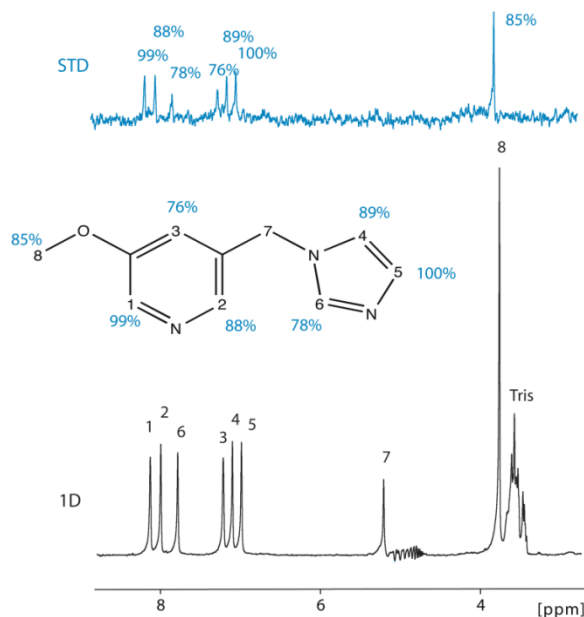


**Figure S4.** Experimental STD data of ligand **15**. The normal 1D-NMR spectrum with 1 mM of ligand **15** in the presence of 10  $\mu$ M DXS is shown in black and the STD spectrum in blue. Saturation was applied for 8 s at  $-0.5$  ppm on a 400 MHz spectrometer (number of scans = 8; temperature = 293 K; time domain = 16384 points).

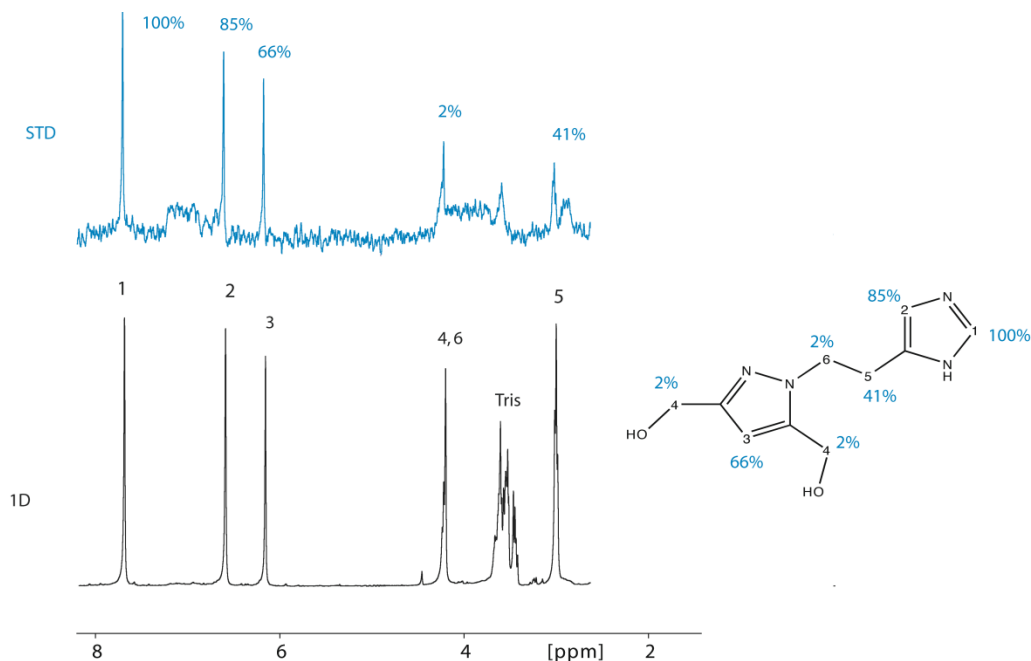


**Figure S5.** Experimental STD data of ligand **16**. The normal 1D with 1 mM of ligand **16** in the presence of 10  $\mu$ M DXS is shown in black and the STD spectrum in blue. Saturation was applied for 8 s on  $-0.5$  ppm on a 700 MHz spectrometer (number of scans = 8; temperature = 293 K; time domain = 16384 points).

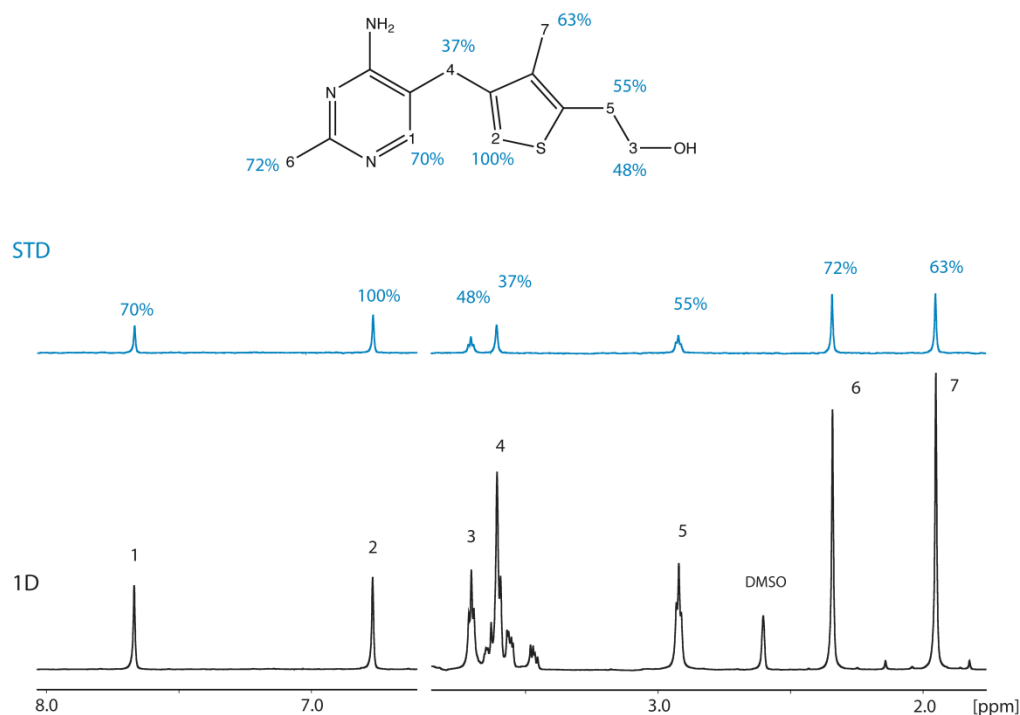


**Figure S6.** Experimental STD data of ligand **17**. The normal 1D-NMR spectrum with 1 mM of ligand **17** in the presence of 10  $\mu$ M DXS is shown in black and the STD spectrum in blue. Saturation was applied for 8 s at  $-0.5$  ppm on a 700 MHz spectrometer (number of scans = 8; temperature = 293 K; time domain = 16384 points).

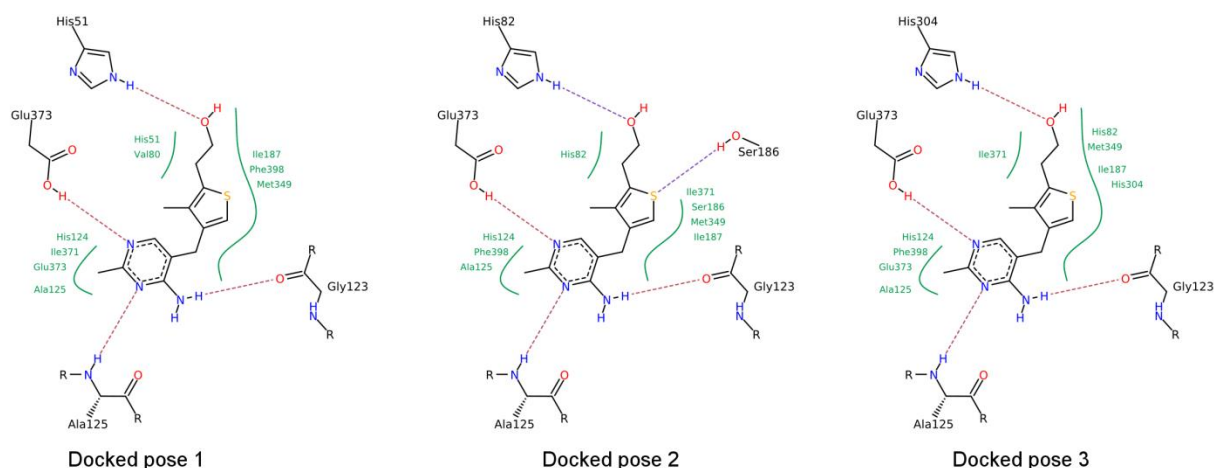


**Figure S7.** Schematic representation of the three top-scoring poses of deazathiamine within *D. radiodurans* DXS (PDB code: 2O1X).<sup>[1]</sup> These binding modes are the result of a docking run using the FlexX docking module with 30 poses and represent the three top-scoring poses after HYDE scoring<sup>[3]</sup> and careful visual inspection to exclude poses with significant inter- or intra-molecular clash terms or unfavourable conformations.  $Mg^{2+}$  has not been included in the docking. The figure was generated with PoseView<sup>[4]</sup> as implemented in the LeadIT suite. This holds also for other figures of this type (Fig. S2, Fig. S3 and Fig. S5). The same protocol was applied for fragments **15**, **16** and **23**.



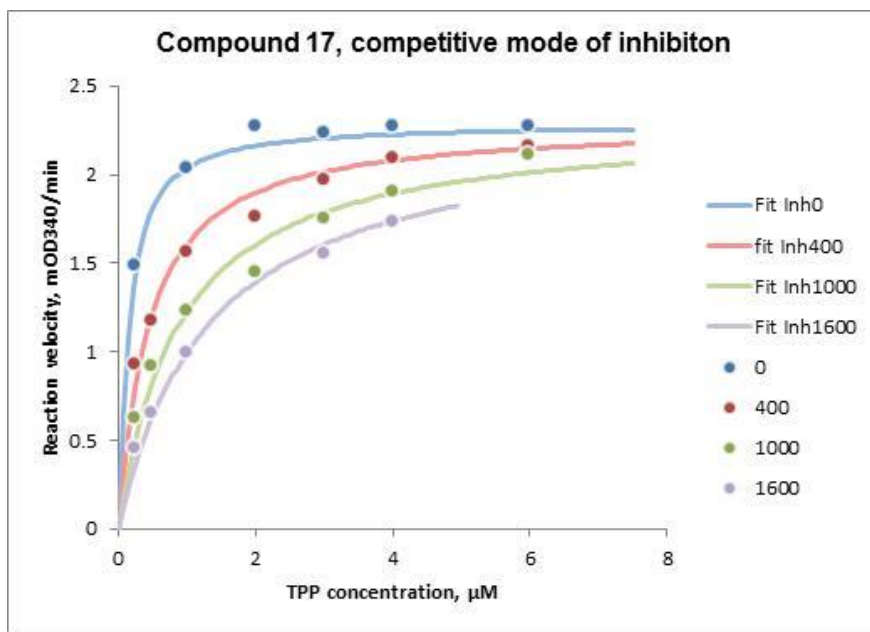


**Figure S8.** Determination of  $K_i$  and mode of inhibition for deazathiamine (**17**).  $K_i$  (competitive mode of inhibition) =  $151 \pm 34 \mu\text{M}$ ; Blue, red, green and grey points represent data sets recorded at concentrations of compound **17** of 0, 400, 1000 and 1600  $\mu\text{M}$ , respectively.

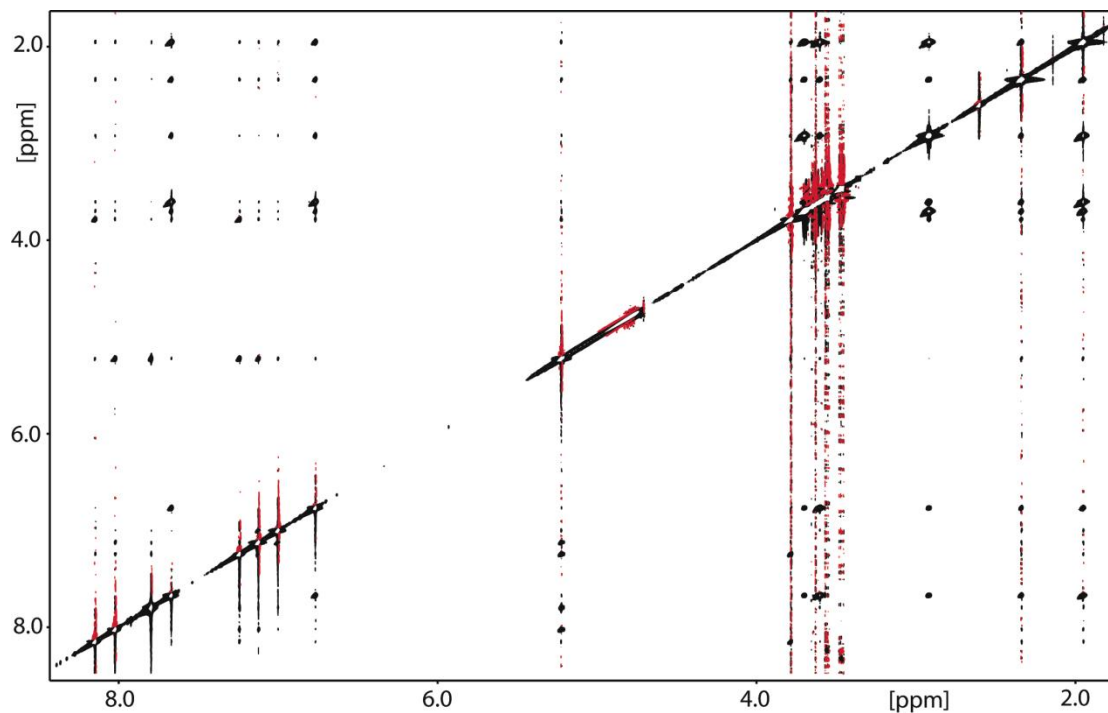


**Figure S9.** NOESY spectrum of inhibitors **15** (1 mM) and **17** (1 mM) in the presence of DXS (30  $\mu$ M) in Tris-HCl buffer. Binding of both ligands to DXS can be clearly seen by the transferred NOE peaks, which have the same sign as the diagonal peaks. INPHARMA peaks between the ligands confirm that they bind to the same binding site. The mixing time was 600 ms on a 700 MHz spectrometer, equipped with a cryogenically cooled probe head. The spectrum was recorded at 293 K with 64 scans, 8192 points in F2 and 640 points in F1.

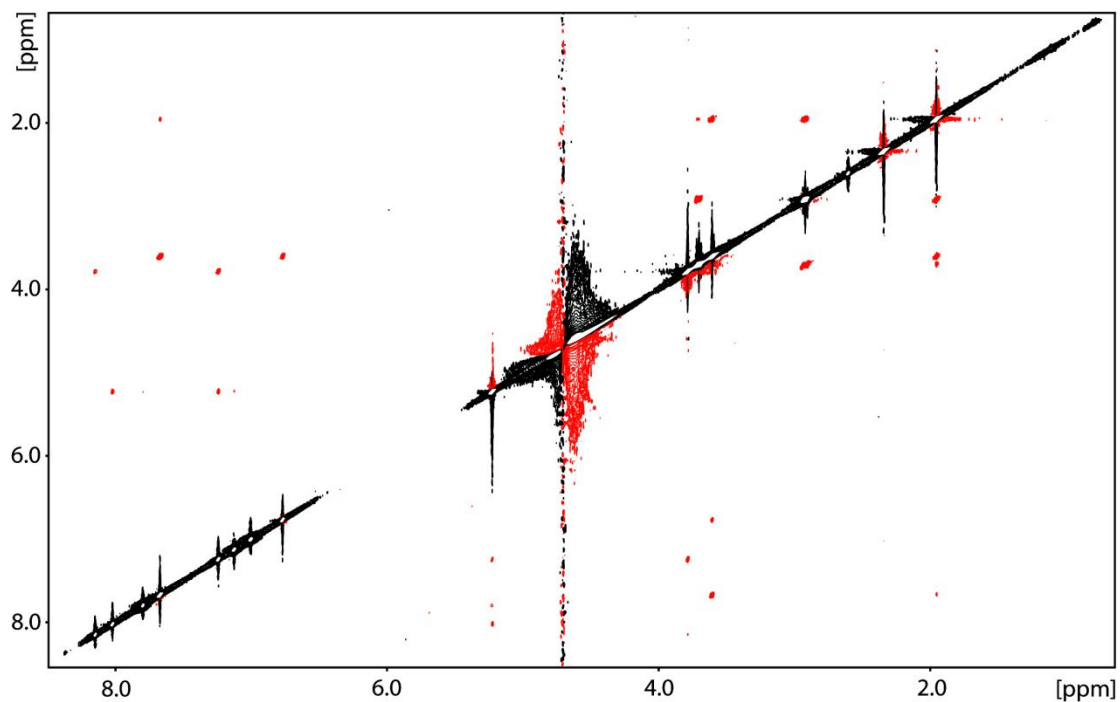


**Figure S10.** NOESY spectrum of inhibitors **15** (1 mM) and **17** (1 mM) in TRIS buffer. No binding is observed and the NOE peaks have the opposite sign as the diagonal peaks. INPHARMA peaks are not observed. The mixing time was 600 ms on a 400 MHz spectrometer. The spectrum was recorded at 293 K with 32 scans, 4096 points in F2 and 256 points in F1.

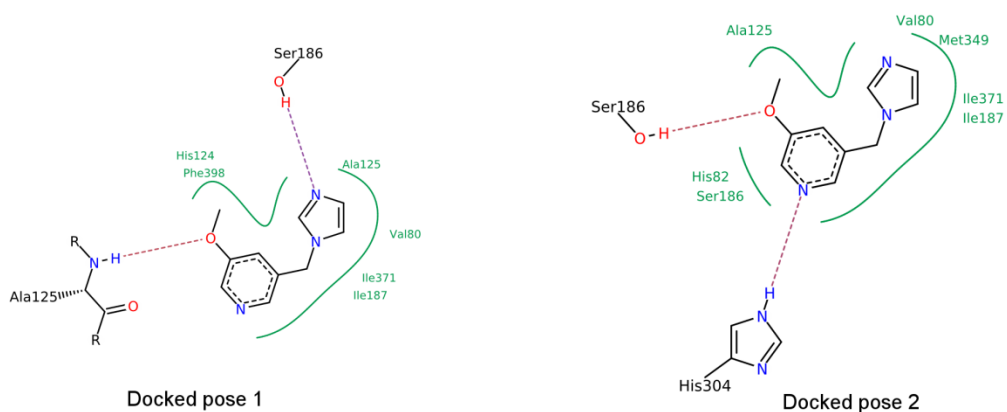


**Figure S11.** Schematic representation of the two top-scoring poses of **15** within *D. radiodurans* DXS.

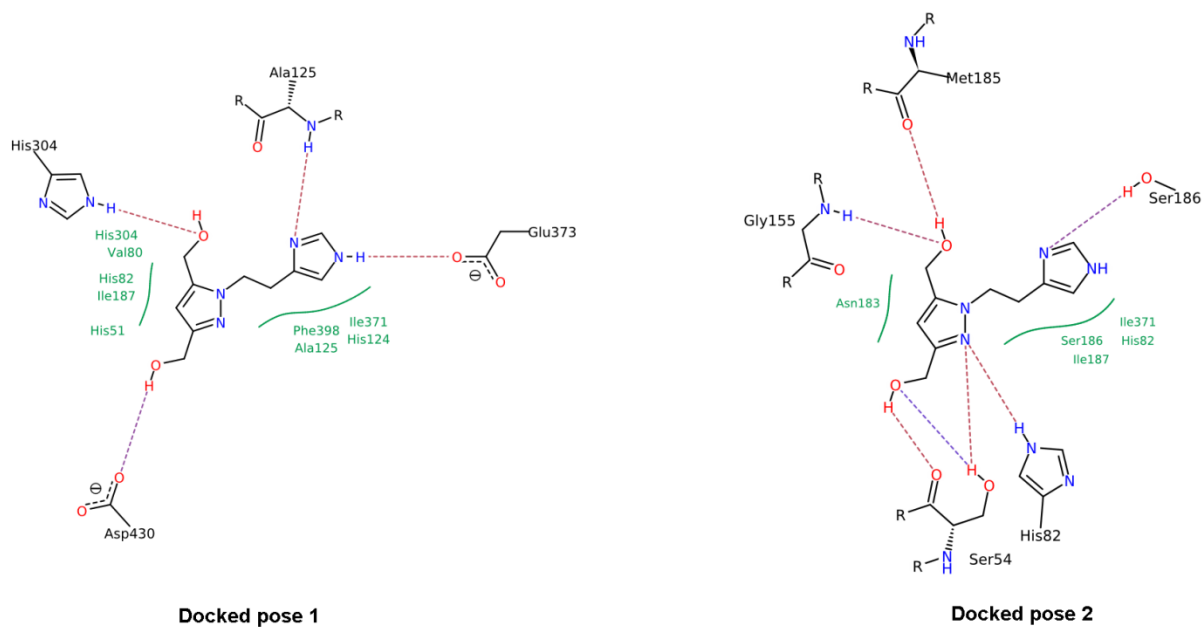


**Figure S12.** Schematic representation of the two top-scoring poses of **16** within *D. radiodurans* DXS.

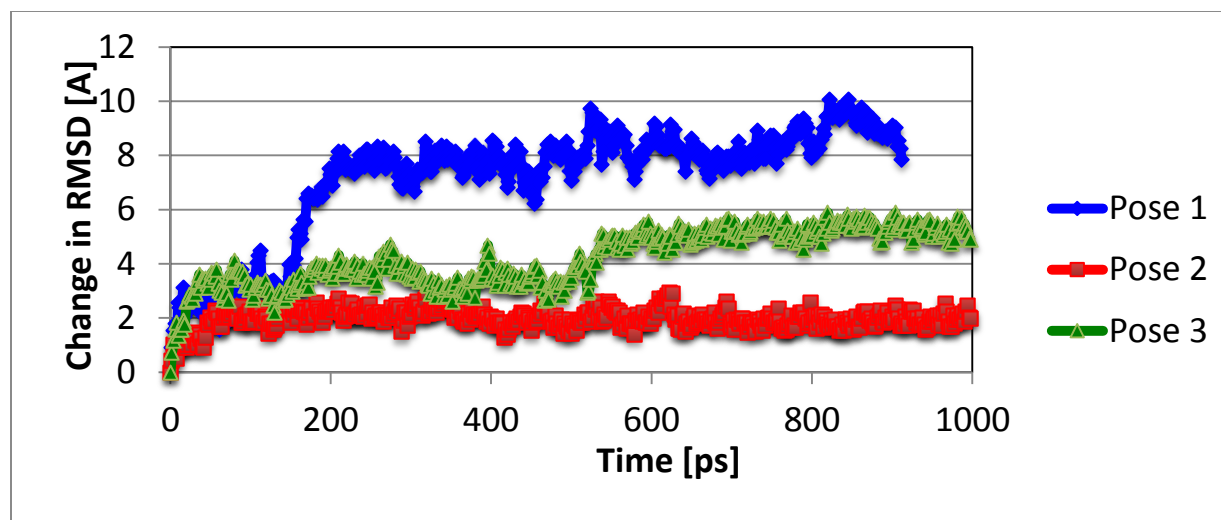


**Figure S13.** The four preferred docking poses of ligand **17** to DXS (poses 1–3) were subjected to a molecular dynamics simulation of 1 ns in implicit solvent. The trajectories and their respective RMSD changes over time are shown above. It is noteworthy that only pose 2 is stable in its binding site (RMSD change only around 2 Å). Binding pose 3 is moving from the starting pose by 4–6 Å RMSD and towards the phosphate-binding site. Binding pose 1 instead completely leaves the binding site. It can therefore be assumed that pose 2 is the most stable binding pose and thus the most probable.

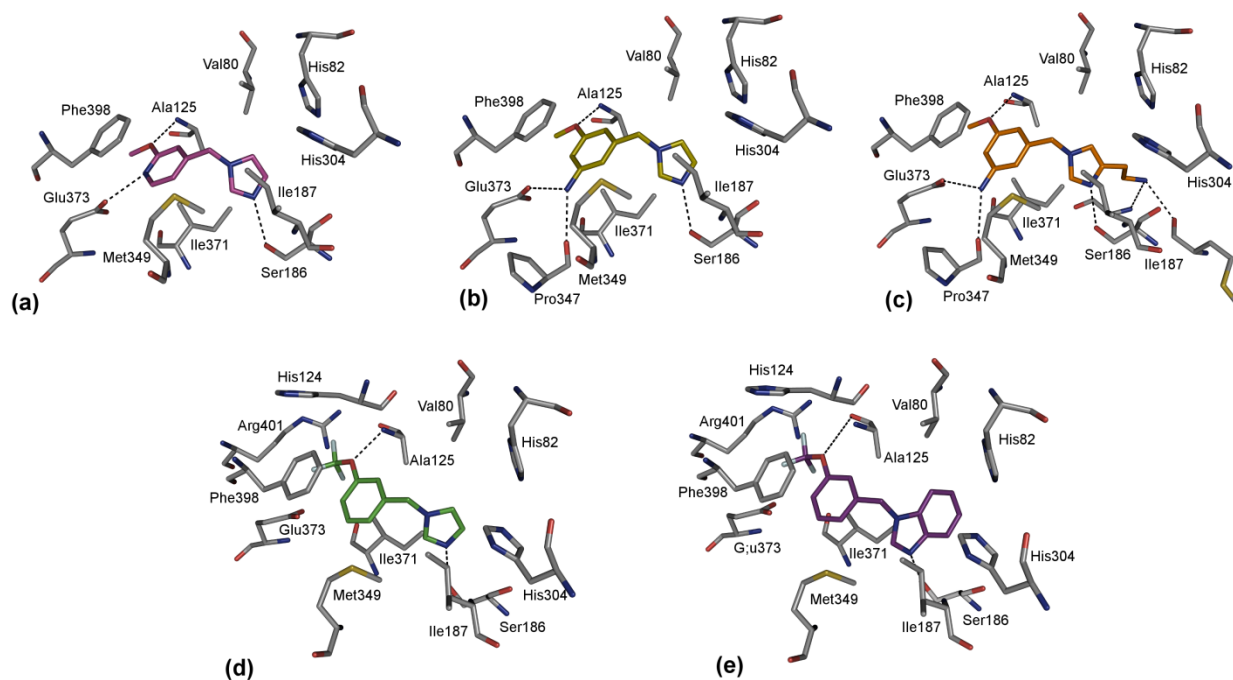


**Figure S14.** Schematic representation of the modelled poses for compounds **19** (a), **20** (b), **21** (c), **22** (d), **23** (e). Modelling was performed using the computer programme MOLOC.<sup>[5]</sup> Colour code: protein skeleton: C: grey; O: red; N: blue; S: yellow. **19**, skeleton: pink; **20**, skeleton yellow; **21**, skeleton orange; **22**, skeleton green, **23**: skeleton purple. The Figure was generated using the software PyMOL.<sup>[6]</sup>

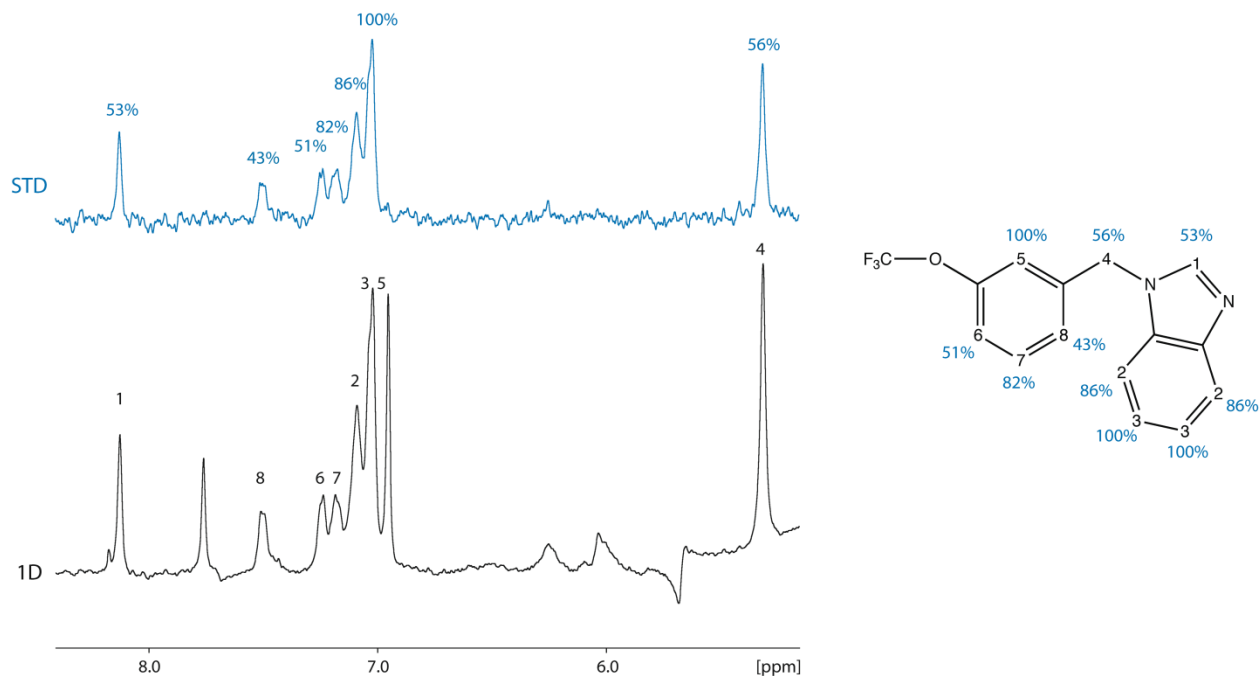


**Figure S15.** Experimental STD data of **23**. The normal 1D-NMR spectrum with 0.5 mM of **23** in the presence of 10  $\mu$ M DXS is shown in black and the STD spectrum in blue. Saturation was applied for 8 s on  $-0.5$  ppm on a 400 MHz spectrometer (number of scans = 8; temperature = 293 K; time domain = 16384 points).

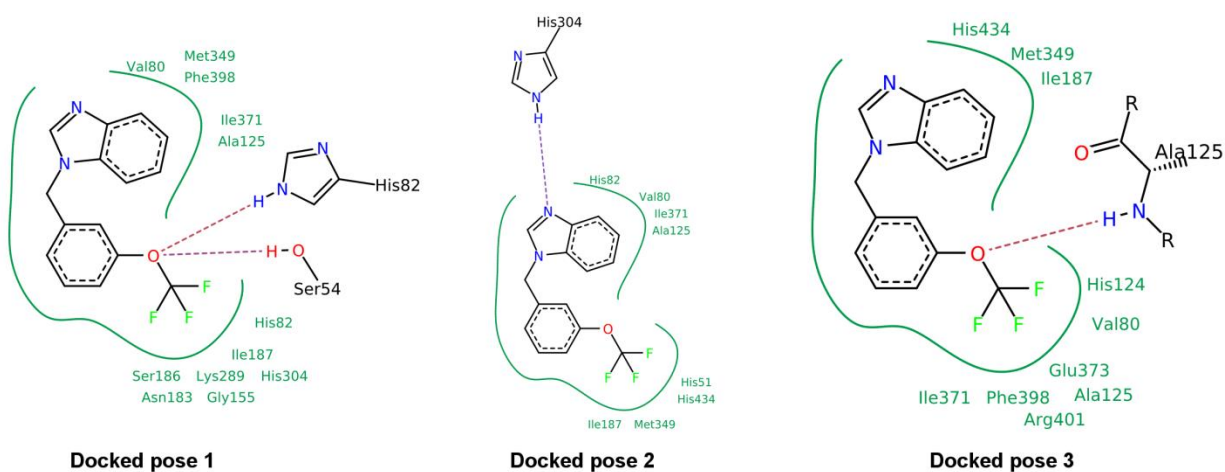


**Figure S16.** Schematic representation of the three top-scoring poses of **23** within *D. radiodurans* DXS.

Compound	Pose <sup>[a]</sup>	$\Delta G_{\text{HYDE}}^{\text{[b]}}$ (kJ.mol <sup>-1</sup> )	R <sub>STI</sub>
<b>15</b>	<i>1</i>	-33	0.52
	<i>2</i>	-18	0.36
<b>16</b>	<i>1</i>	-22	0.42 <sup>[c]</sup>
	<i>2</i>	-8	0.45 <sup>[c]</sup>
<b>17</b>	<i>1</i>	-38	-
	<i>2</i>	-32	-
	<i>3</i>	-39	-
<b>23</b>	<i>1</i>	-11	0.40
	<i>2</i>	-20	0.46
	<i>3</i>	-23	0.57

[a] The numbers of each pose refer to the representative poses obtained from the docking studies, shown in Fig. S1, S2, S3 and S5. A representative pose for every different binding mode has been taken into account, with the highest binding energy.

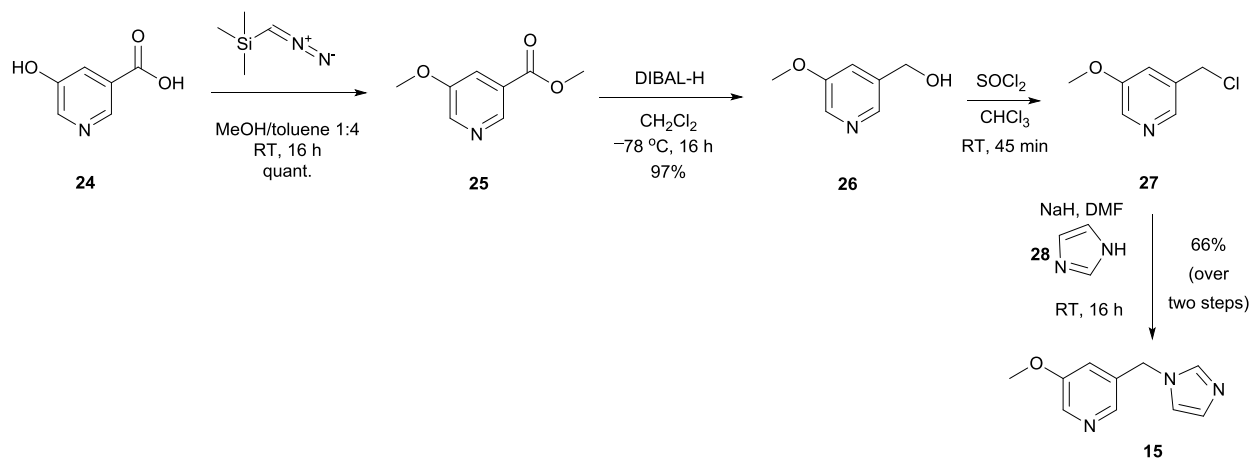
[b] Values indicate the calculated Gibbs free energy of binding ( $\Delta G_{\text{HYDE}}$ ; calculated by the HYDE scoring function in the LeadIT suite).<sup>[2]</sup>

[c] R<sub>ST</sub> values reported, given that no peaks were observed in the INPHARMA measurement.

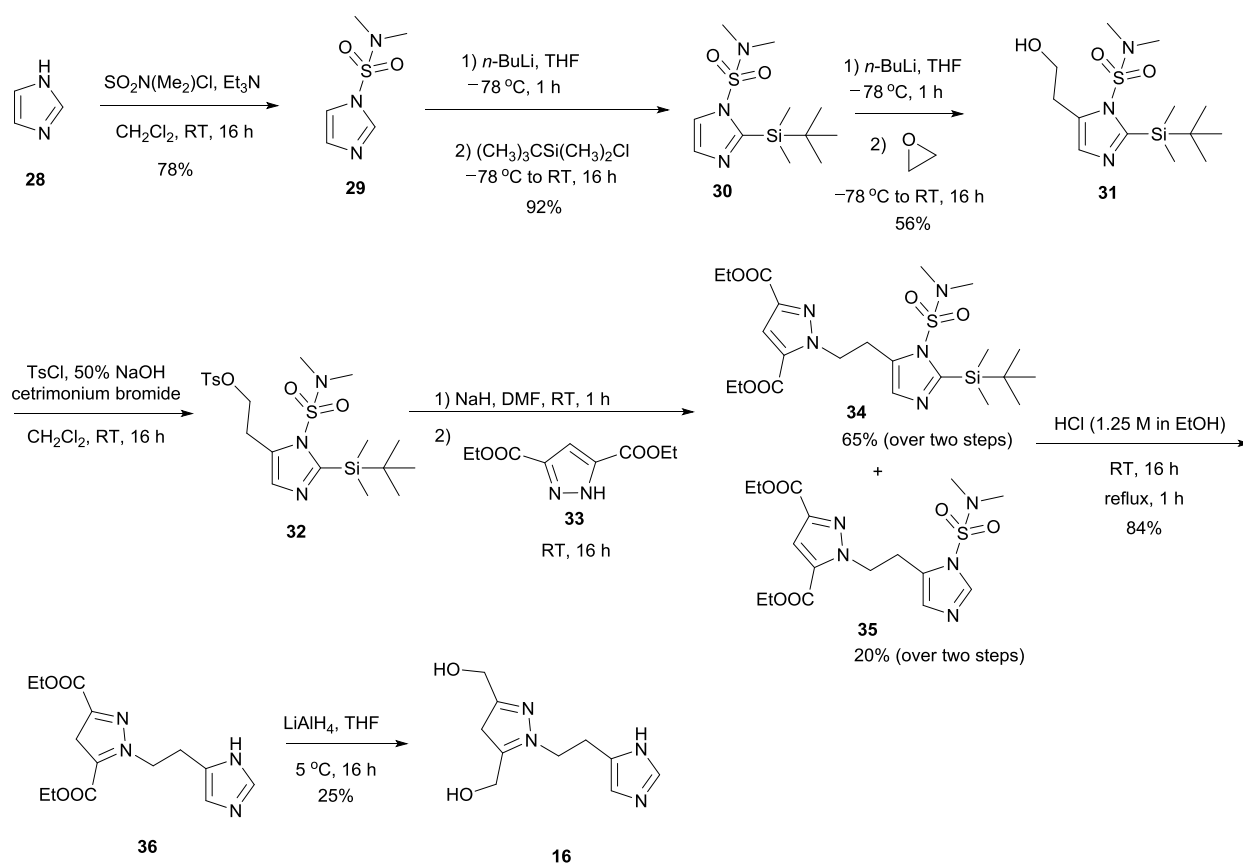
**Table S1.** Calculated Gibbs free energy of binding and corresponding R<sub>STI</sub> values of deazathiamine (**17**) and of the modelled compounds **15**, **16** and **23**.



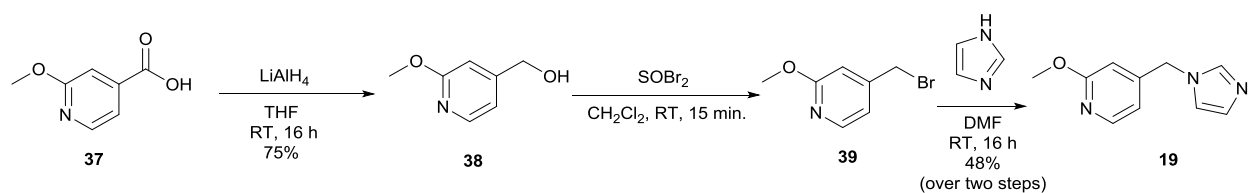
## Synthetic schemes for the synthesis of compounds 15, 16, 19–23



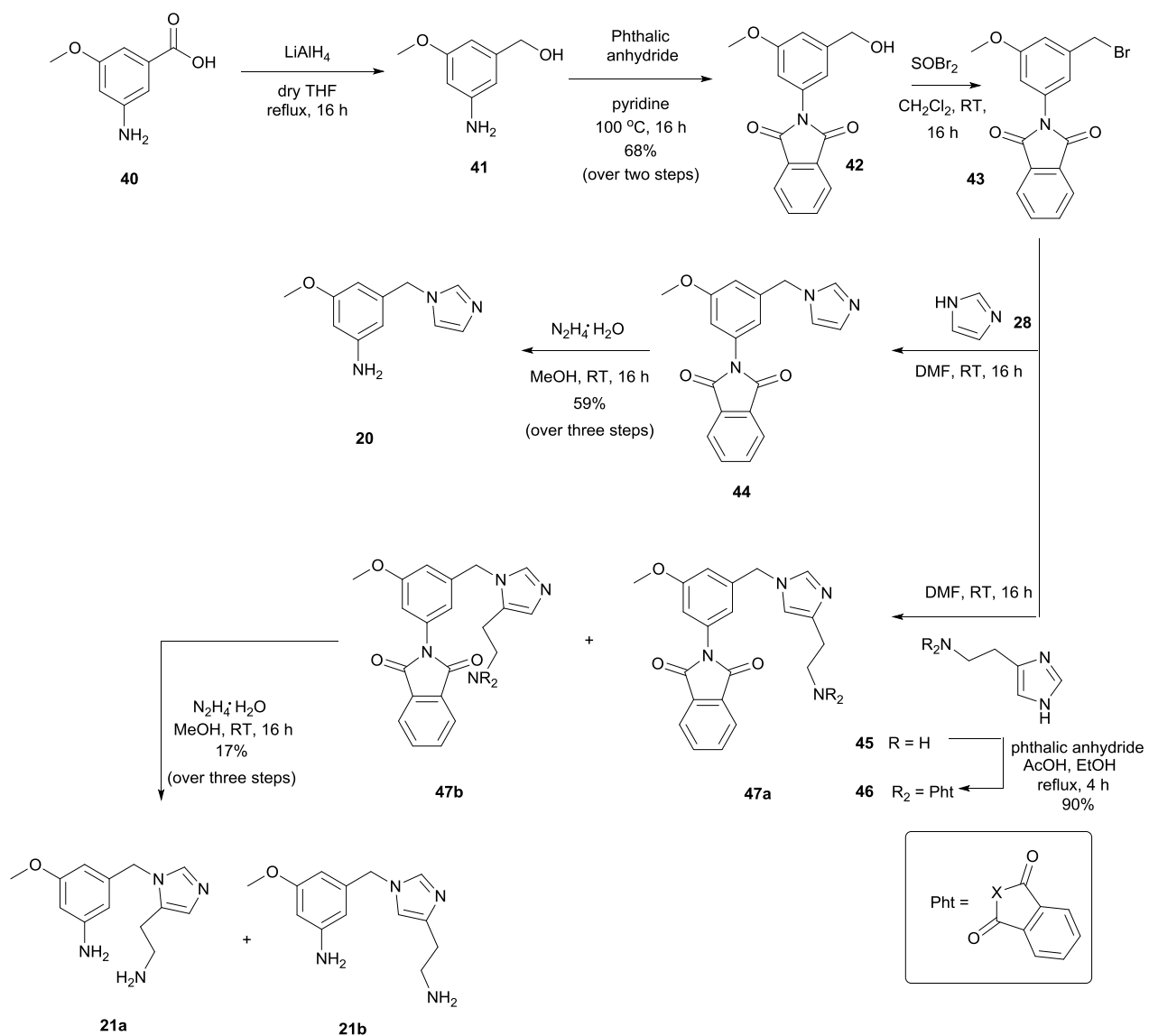
**Scheme S1.** Synthesis of fragment **15**.



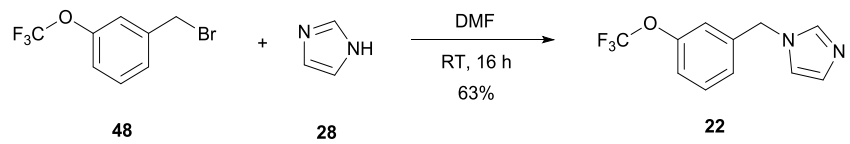
**Scheme S2.** Synthesis of fragment **16**.



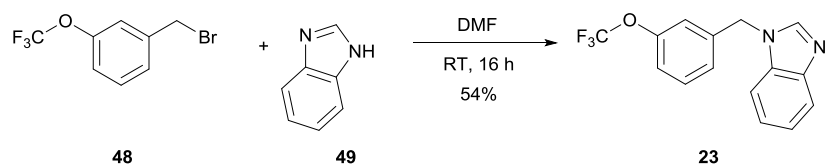
**Scheme S3.** Synthesis of fragment **19**.



**Scheme S4.** Synthesis of fragments **20** and **21a** and **21b** as a mixture of the two regioisomers.



**Scheme S5.** Synthesis of fragment **22**.



**Scheme S6.** Synthesis of fragment **23**.

## Modelling and Docking

The X-ray crystal structure of *D. radiodurans* DXS in complex with TDP (PDB code: 2O1X) was used for our modelling.<sup>[1]</sup> Fragments **15**, **16**, **19–23** were designed so as to occupy the TDP-binding pocket. The energy of the system was minimised using the MAB force field as implemented in the computer programme MOLOC,<sup>[5]</sup> whilst keeping the protein coordinates fixed. After energy minimisation of the designed fragments, all types of interactions (hydrogen bonds and lipophilic interactions) between the fragments and the protein were analysed in MOLOC. Compounds **15**, **16**, **23** and deazathiamine (**17**) were generated using the three-dimensional structure generator software CORINA<sup>[7]</sup> and protonated with FCONV<sup>[8]</sup> and subsequently docked into the TDP-binding pocket of *D. radiodurans* DXS by using the FlexX docking module in the LeadIT suite.<sup>[2]</sup> To define a binding pocket for docking, we applied a standard procedure resulting in an enclosing volume utilising the co-crystallized ligand TDP defined as the “reference ligand”. Every protein atom within a distance of 11 Å from any reference-ligand atom, was defined to be part of the binding site for FlexX. Given that the docking algorithm may deliver more than one pose per docking run, a maximum of 30 FlexX-scored solutions were retained, and subsequently re-scored with the HYDE<sup>[3]</sup> module in LeadIT v.2.1.2. After careful visualisation to exclude poses with significant inter- or intramolecular clash terms or unfavourable conformations and analysis of the selected poses with the programme torsion analyser,<sup>[9]</sup> the resulting solutions were subsequently ranked according to their free energies of binding. A representative pose for every different binding mode with the highest binding energy was taken into account and was used to support the NMR studies.

## **Construction of Expression Vectors pET22b-H6TBKDRDXS and pET22b-H6TEVEKMTDXS**

A gene containing an N-terminal sequence encoding a hexahistidine tag and cleavage sites for TEV protease and enterokinase was adapted to the codon usage of *Escherichia coli* and has been synthesised by the custom synthesis service of GenScript (GenScript USA Inc., NJ, USA) and cloned into the expression vector pET22b<sup>+</sup> by NdeI and HindIII. The resulting plasmids were electroporated into *E. coli* BL21(DE3) cells, affording the recombinant strains BL21(DE3)-pET22b-H6TEVEKDRDXS (acc. no. KJ462005; *D. radiodurans*) and BL21(DE3)-pET22b-H6TEVEKMTDXS (acc. no. KJ462006; *M. tuberculosis*).

### **Purification of DXS from *D. radiodurans* and *M. tuberculosis***

Cells of *E. coli* BL21(DE3) carrying plasmid pET22b-H6TEVEKDRDXS (for *D. radiodurans* DXS) or pET22b-H6TEVEKMTDXS (for *M. tuberculosis* DXS) were inoculated into LB medium supplemented with ampicillin (100 mg/mL) and cultivated in shaking flasks at 37 °C until OD<sub>590</sub> = 0.4. IPTG was added to 0.5 mM, and the cell culture was further incubated at 20 °C for 20 h. Cells were harvested by centrifugation (4000 rpm, 40 min, 4 °C), washed once with aq. NaCl solution (0.9%) and resuspended in buffer A (50 mM Tris-HCl pH 8.0, 300 mM NaCl, 15 mM imidazole, 0.02% NaN<sub>3</sub>), 5 mL per 1 g of cells. Cells in buffer A were disrupted with French-Press, debris was removed by centrifugation, and the supernatant was applied to a Ni-chelating sepharose column (1 cm x 15 cm) equilibrated with buffer A. The column was washed with buffer A until OD<sub>280</sub> of the effluent came back to the base line and then developed with the gradient of imidazole (15 mM – 800 mM). Fractions containing DXS were combined, transferred to buffer B (50 mM Tris-HCl pH 8.0, 100 mM NaCl, 5 mM DTT, 0.02% NaN<sub>3</sub>) using desalting column HiPrep 26/10 Desalting (GE Healthcare), concentrated to 19 mg/mL (*D. radiodurans* DXS) or 1.1 mg/mL (*M. tuberculosis* DXS) using Amicon Stirred Ultrafiltration Cell (Amicon) equipped with polyethersulfone ultrafiltration membrane (pore size 10 kDa, Pall Life Sciences) and frozen at –80 °C for long-term storage. Isolated and purified DXS showed no measurable DXS activity unless enough external TDP was added.

## Photometric assay for kinetic studies of DXS

Photometric assays were conducted in transparent flat-bottomed 96-well plates (Greiner Bio-One). Assay mixtures contained 100 mM Tris-HCl (pH 7.6), 4 mM MnCl<sub>2</sub>, 5 mM dithiothreitol (DTT), 0.5 mM NADPH, 1.2 μM TDP, 0.5 mM sodium pyruvate, 1.0 mM glyceraldehyde 3-phosphate, 8.3 μM IspC and 0.41 μM *D. radiodurans* DXS.

The tolerance of DXS with respect to DMSO concentration was determined by measurement of the reaction velocity in the presence of different concentrations of DMSO. The activity of the enzyme was found to be stable in presence of up to 3% DMSO.

The potential inhibitors for DXS were dissolved in DMSO so as to get 160 mM solutions when possible. Their solubility in the assay buffer was tested prior to the inhibitory assay so as to get 2000 μM as the highest concentration tested when possible. Dilution series of the compounds tested typically covered the concentration range of 2000 μM to 4.0 μM. The concentration range varied depending on the solubility of the organic molecule in DMSO and in the assay buffer.

The reaction was started by adding 95 μL of buffer A (100 mM Tris-HCl (pH 7.6), 8 mM MnCl<sub>2</sub>, 10 mM dithiothreitol (DTT), 1.0 mM NADPH, 2.4 μM TDP, 1.0 mM sodium pyruvate, 4.1 μM IspC and either 0.82 μM *D. radiodurans* DXS or 4.0 μM *M. tuberculosis* DXS) to 95 μL of a buffer solution (100 mM Tris-HCl (pH 7.6) containing the DMSO solution of inhibitor and glyceraldehyde 3-phosphate (2 mM). The reaction was monitored photometrically at room temperature at 340 nm using either a Synergy Mx (Biotek) or SpectraMax M5 (Molecular Dynamics) microplate reader. Initial rate values were evaluated with a nonlinear regression method using the program Dynafit.<sup>[10]</sup>

The dissociation constant ( $K_d$ ) for TDP-DXS complex was determined as follows. Dilution series (1:2) of TDP, covering the concentration range of 60 μM to 0.02 μM were prepared in buffer A (100 μL per test well). The reaction was started by adding 100 μL buffer B that did not contain TDP. The  $K_d$  values for TDP determined from the best fit of data to the reaction model with the programme Dynafit<sup>[10]</sup> are  $114 \pm 13$  nM (*D. radiodurans* DXS) and  $3.1 \pm 0.3$  μM (*M. tuberculosis* DXS). The reaction model used for the data fit, included a series of reaction steps:

$E + T \rightleftharpoons ET$  (reversible binding of TDP to the apoDXS,  $K_d$  is a TDP dissociation constant for this reaction step);

$E + S \rightleftharpoons ES$  (reversible binding of one of the substrates to the apoDXS,  $K_s$  is a substrate dissociation constant for this reaction step);

$ET + S \rightleftharpoons ETS$  (reversible binding of one of the substrates to the holoDXS,  $K_s$  is a substrate dissociation constant for this reaction step);

$ETS \rightarrow ET + P$  (irreversible conversion of ETS complex to the holoDXS and reaction product DXP (P),  $k_{cat}$  is a reaction constant for this reaction step).

The mode of inhibition for compound **17** was determined as described as follows. As in the assay for  $IC_{50}$  determination, reaction mixtures contained 100 mM Tris-HCl (pH 7.6), 4 mM  $MnCl_2$ , 5 mM DTT, 0.5 mM NADPH, 0.5 mM sodium pyruvate, 2.05  $\mu M$  IspC and 0.41  $\mu M$  *D. radiodurans* DXS. Both concentration of inhibitor and TDP were varied in the assay, giving the following concentration windows: inhibitor: 0–2000  $\mu M$ ; TDP: 0.25–6  $\mu M$ . The reaction was started by the addition of glyceraldehyde 3-phosphate to a final concentration of 1.0 mM. The velocity-TDP data were fitted for all inhibitor concentrations with a nonlinear regression method using the programme DynaFit.<sup>[10]</sup> Three inhibition models (competitive, uncompetitive and mixed) were considered for the calculation.  $K_i$  and  $K_{is}$  values, defined as inhibition constants for competitive and uncompetitive modes of inhibition, respectively, were obtained from the fit under consideration of the most likely inhibition model as described earlier.<sup>[11]</sup>

### Calculation of $K_i$ values

For the calculation of the  $K_i$  values with the programme Dynafit<sup>[10]</sup>, the same data set as for the  $IC_{50}$  evaluation was used, and a model for competitive inhibition was applied, which can be described as a series of several processes that can be included in the script file for Dynafit as follows:

$E + T \rightleftharpoons ET$  (reversible binding of TDP to the apoDXS,  $K_d$  is a dissociation constant for TDP);

$E + S \rightleftharpoons ES$  (reversible binding of one of the substrates to the apoDXS,  $K_s$  is a dissociation constant for the substrate);

$ET + S \rightleftharpoons ETS$  (reversible binding of one of the substrates to the holoDXS,  $K_s$  is a dissociation constant for substrate);

$E + I \rightleftharpoons EI$  (reversible binding of inhibitor to the apoDXS,  $K_i$  is a dissociation constant for inhibitor);

$EI + S \rightleftharpoons EIS$  (reversible binding of one of the substrates to the apoDXS/inhibitor complex,  $K_s$  is a dissociation constant for respective substrate);

$ETS \rightarrow ET + P$  (irreversible conversion of ETS complex to the holoDXS and reaction product DXP (P),  $k_{cat}$  is a reaction constant for this process).

As a result, the  $K_i$  values determined this way describe the inhibitory potency of a particular compound under analysis.  $K_s$  and  $K_d$  values for the target enzyme in the assay must be determined separately in advance and used for  $K_i$  determination as unchangeable parameters. For reasons of simplicity, a model that includes only one substrate species (pyruvate) was used given that a model with two substrate species (pyruvate and glyceraldehyde 3-phosphate) afforded the same  $K_s$  values as the model with one substrate species.

### **Experimental procedures for the NMR and STI cross validation of the docking poses**

Sample preparation: 380  $\mu\text{L}$   $\text{D}_2\text{O}$  Tris-buffer with a DXS concentration of 30  $\mu\text{M}$  were combined with 1 mM ligand concentration and 20  $\mu\text{L}$  DMSO- $d_6$ . In the case of ligand **23**, the concentration was 0.5 mM, due to the low solubility of the ligand.

NMR experiments: The NOESY spectra were recorded on a 700 MHz or 800 MHz spectrometer equipped with cryogenically cooled probe (Bruker, Karlsruhe), using a standard pulse sequence with a mixing time of 600 ms. STD spectra were recorded with a standard pulse sequence (stdiffesgp.2) on a 400 MHz spectrometer. Number of scans and points in the time domain are given in the corresponding captions of each figure. Saturation was achieved by a train of shaped  $90^\circ$  pulses of 50 ms length. A number of 160 selective pulses was applied, leading to a total length of saturation of 8 s. The on-resonance irradiation was performed at  $-0.5$  ppm and off-resonance irradiation was set to  $+30$  ppm.

Back-calculation of peak volumes: INPHARMA, trNOE and STD peak volumes were back-calculated with the software SpINPHARMA ([www.inpharma.de](http://www.inpharma.de)). STD saturation was applied to all methyl groups of the protein. Protons within a distance of 8 Å from any ligand proton were considered. The correlation time of DXS was estimated to be 100 ns (molecular weight: 68 kDa plus dimer formation).  $K_d$  values were based on the measured  $\text{IC}_{50}$  values. On-rates ( $k_{\text{on}}$ ) were assumed to be in the diffusion limit  $10^8 \text{ M}^{-1}\text{s}^{-1}$ .

### **Procedures for the MD simulations**

Energy minimisation (EM) and molecular dynamics (MD) simulations were done as implemented in Gromacs<sup>[12]</sup>, using the amber99sb force field<sup>[13]</sup> for the protein and the General Amber Force



Field<sup>[14]</sup> for the ligand in implicit solvent (GBSA). EM was done with conjugate gradient integrator in 1000 steps. MD was done using stochastic dynamics integrator with a stepsize of 2 fs.

## Experimental Procedures

### General Experimental Details

Starting materials and reagents were purchased from Aldrich, Acros, Alfa Aesar or Apollo Scientific. Yields refer to analytically pure compounds and have not been optimised. All solvents were reagent-grade and if necessary, dried and distilled prior to use. All reactions were run under a nitrogen atmosphere unless otherwise stated. Column chromatography was performed using silica gel (Silicycle<sup>®</sup> SiliaSep<sup>™</sup> 40–63  $\mu\text{m}$ ). TLC was performed with silica gel 60/Kieselguhr F254. Solvents used for the column chromatography were dichloromethane, methanol, ethylacetate or pentane. <sup>1</sup>H-NMR and <sup>13</sup>C-NMR spectra were recorded at 400 MHz on a Varian AMX400 spectrometer (400 MHz for <sup>1</sup>H, 101 Hz for <sup>13</sup>C) at 25 °C. Chemical shifts ( $\delta$ ) are reported relative to the residual solvent peak (CHCl<sub>3</sub>, <sup>1</sup>H = 7.24; <sup>13</sup>C = 77.23. CD<sub>3</sub>OD, <sup>1</sup>H = 3.31; <sup>13</sup>C = 49.15). Splitting patterns are indicated as (s) singlet, (d) doublet, (t) triplet, (q) quartet, (m) multiplet, (br) broad. High resolution mass spectra were recorded with an LTQ Orbitrap XL (Thermo Fisher Scientific) mass spectrometer, using ESI (or APCI or APPI) as ionization source. FT-IR were measured on PerkinElmer FT-IR spectrometer. Melting points were measured with a Buchi melting point B-545. HPLC conditions for **23**: column Waters Xterra MS C8 AD-RH 5  $\mu$ , 150 mm  $\times$  4.6 mm; flow rate 0.5 mL min<sup>-1</sup>; wavelength 265 nm; temperature 23 °C; gradient method, acetonitrile (0.1% TFA)/water (0.1% TFA) 10:90 to 95:5 for 65 minutes. HPLC conditions for **20**: column Astec Chirobiotic T 5  $\mu$ , 250 mm  $\times$  4.6 mm; flow rate 0.5 mL min<sup>-1</sup>. Deazathiamine (**17**),<sup>[15]</sup> deazathiamine diphosphate (**18**),<sup>[15]</sup> **29**,<sup>[16]</sup> **30**,<sup>[17]</sup> **31**,<sup>[18]</sup> **38**,<sup>[19]</sup> **39**,<sup>[19]</sup> and **46**<sup>[20]</sup> were synthesized according to known literature procedures.

## Synthesis

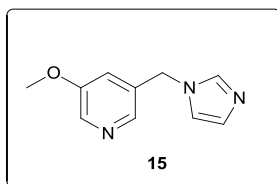
### General procedure for S<sub>N</sub>2 reaction (GP1)

To a solution of the nucleophile (1 eq.) in dry DMF (1.0 mL per 0.15 mmol) at 0 °C, the electrophile (benzyl chloride or benzyl bromide, 1–1.2 eq.) was added dropwise. The reaction mixture was left to warm up and stir at room temperature for 16 h. DMF was removed *in vacuo*, and the residue was purified by column chromatography.



## General procedure for phthalimide deprotection (GP2)

A solution of the phthalimide-protected amine (1 eq.) in MeOH (1.0 mL per 0.017 mmol) was treated with  $\text{N}_2\text{H}_4 \cdot \text{H}_2\text{O}$  (50–60% solution, 11.4–17.0 eq.), and the mixture was left to stir at room temperature for 16 h. MeOH was removed *in vacuo* and the crude was extracted with EtOAc (3x), the organic layers dried over  $\text{Na}_2\text{SO}_4$ , filtered and concentrated *in vacuo*. Alternatively, the crude was dissolved in water and the solution acidified (according to pH paper) by adding aq. HCl (1N); the aqueous layer was extracted with EtOAc (3x) and subsequently basified by treatment with aq. NaOH (1N) (according to pH paper). After extraction with EtOAc (3x) and DCM/iPrOH (3:1, 3x), the organic layers were concentrated *in vacuo*. The residue was purified by column chromatography.



### 3-((1*H*-Imidazol-1-yl)methyl)-5-methoxypyridine (15)

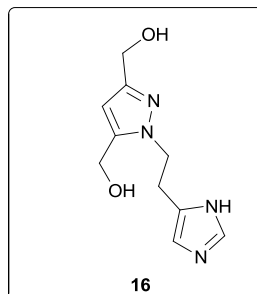
A dry flask was charged with imidazole (**28**) (12.4 mg, 0.18 mmol, 1.0 eq.) and anhydrous DMF (1.0 mL). NaH (60% dispersion in mineral oil, 14.6 mg, 0.4 mmol, 2.0 eq.) was added, and the mixture was stirred at room temperature for 1 h. **27** (38.4 mg, 0.20 mmol, 1.1 eq.) was added, and the mixture was allowed to stir at room temperature for 16 h. The solvent was removed *in vacuo*, and the crude was purified by CC ( $\text{SiO}_2$ ;  $\text{CH}_2\text{Cl}_2/\text{MeOH}$ , 1:4) to afford **15** as a yellow oil (22.5 mg, 66%).

$^1\text{H}$  NMR (400 MHz,  $\text{CDCl}_3$ ):  $\delta$ =8.25 (d, 1H,  $J$ =2.7 Hz), 8.10 (d, 1H,  $J$ =1.6 Hz), 7.54 (s, 1H), 7.09 (s, 1H), 6.88 (s, 1H), 6.85 (s, 1H), 5.10 (s, 2H), 3.79 (s, 3H).

$^{13}\text{C}$  NMR (101 MHz,  $\text{CDCl}_3$ ):  $\delta$ = 155.96, 140.67, 137.71 (2C), 132.38, 130.31, 119.13 (2C), 55.62, 48.08.

HR-MS (ESI) calcd for  $\text{C}_{10}\text{H}_{12}\text{N}_3\text{O}$  [ $M+\text{H}$ ] $^+$ : 190.0975; found: 190.0982.

IR: 3118.2, 3058.2, 2925.9, 2623.6, 1669.6, 1592.4, 1472.2, 1432.9, 1292.9, 1198.8, 1129.4, 1052.8, 1018.2, 877.9, 828.9, 799.2, 759.4, 719.9, 703.8, 636.9, 598.3, 588.7, 543.6, 518.9.



**(1-(2-(1H-Imidazol-5-yl)ethyl)-1H-pyrazole-3,5-diyl)dimethanol (16)**

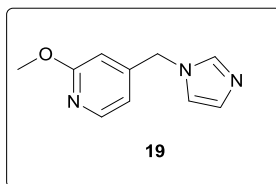
A suspension of  $\text{LiAlH}_4$  (16 mg, 0.42 mmol, 3.2 eq.) in anhydrous THF (2 mL) was cooled to 5 °C. A solution of **36** (40 mg, 0.13 mmol, 1.0 eq.) in anhydrous THF (1.5 mL) was added dropwise, and the mixture was stirred at 5 °C for 36 h. The mixture was quenched with sequential addition of  $\text{H}_2\text{O}$  (0.016 mL), NaOH (15% aq. solution; 0.032 mL) and  $\text{H}_2\text{O}$  (0.048 mL), filtered through paper, and the filter washed with MeOH (3 mL). The filtrate was concentrated *in vacuo*, and the residue was purified by CC ( $\text{SiO}_2$ ;  $\text{CHCl}_3/\text{MeOH}/\text{H}_2\text{O}$ , 5:5:1) to afford **16** as a colourless oil (29 mg, quant.).

$^1\text{H}$  NMR (400 MHz,  $\text{CD}_3\text{OD}$ ):  $\delta$ =7.64 (s, 1H), 6.72 (s, 1H), 6.19 (s, 1H), 4.54 (s, 2H), 4.37 (s, 2H), 4.33 (t, 2H,  $J$ =7.1 Hz), 3.09 (t, 2H,  $J$ =7.1 Hz).

$^{13}\text{C}$  NMR (101 MHz,  $\text{CD}_3\text{OD}$ ):  $\delta$  153.03, 145.15, 136.29, 135.55, 118.16, 105.16, 58.99, 55.40, 50.25, 29.19.

HR-MS (ESI) calcd for  $\text{C}_{10}\text{H}_{15}\text{N}_4\text{O}_2$  [ $M+\text{H}$ ] $^+$ : 223.11895, found: 223.11870.

IR: 3203.9, 2919.7, 2876.9, 1680.1, 1570.2, 1455.5, 1434.7, 1403.6, 1359.5, 1317.0, 1204.0, 1179.3, 1139.5, 1086.1, 1017.4, 953.4, 801.2, 720.9, 661.2, 624.1.



#### 4-((1*H*-Imidazol-1-yl)methyl)-2-methoxypyridine (**19**)

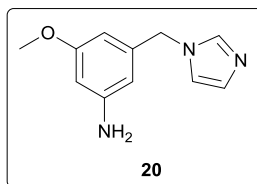
Compound **19** was synthesised according to GP1, starting from **39** (15.2 mg, 0.075 mmol) and imidazole (**28**) (5.1 mg, 0.075 mmol) in anhydrous DMF (0.5 mL). The mixture was stirred at room temperature for 16 h and concentrated *in vacuo*. Purification by CC (SiO<sub>2</sub>; 4% MeOH in CH<sub>2</sub>Cl<sub>2</sub>) afforded **19** as a transparent oil (5.8 mg, 48% yield over two steps).

<sup>1</sup>H NMR (400 MHz, CDCl<sub>3</sub>): δ=8.11 (d, 1H, *J*=5.3 Hz), 7.63 (s, 1H), 7.13 (s, 1H), 6.90 (s, 1H), 6.59 (d, *J*=5.3 Hz, 1H), 6.43 (s, 1H), 5.08 (s, 2H), 3.90 (s, 3H)

<sup>13</sup>C NMR (101 MHz, CDCl<sub>3</sub>): δ=165.06, 148.09, 147.89, 137.83, 130.28, 119.68, 114.96, 180.98, 53.79, 49.70.

HR-MS (ESI) calcd for C<sub>10</sub>H<sub>11</sub>N<sub>3</sub>O [*M*+H]<sup>+</sup>: 190.0975, found: 190.0975.

IR (cm<sup>-1</sup>): 3379.33, 3111.50, 2948.67, 1614.15, 1564.85, 1450.66, 1399.11, 1316.03, 1292.34, 1230.37, 1154.59, 1044.26, 990.05, 816.95, 774.42, 750.51, 663.16.



### 3-((1H-Imidazol-1-yl)methyl)-5-methoxyaniline (**20**)

Compound **20** was synthesised according to GP2, starting from **44** (5.7 mg, 0.017 mmol) and  $\text{N}_2\text{H}_4 \cdot \text{H}_2\text{O}$  (50–60 % solution, 19.4  $\mu\text{L}$ , 0.194 mmol) in MeOH (1.0 mL). Purification by CC( $\text{SiO}_2$ ;  $\text{CH}_2\text{Cl}_2/\text{MeOH}$ , 95:5 to  $\text{CH}_2\text{Cl}_2/\text{MeOH}$ , 92:8) afforded **20** as a white solid (3.5 mg, 59% over two steps).

$^1\text{H}$  NMR (400 MHz,  $\text{CDCl}_3$ ):  $\delta$ =7.55 (s, 1H), 7.08 (s, 1H), 6.91 (s, 1H), 6.14 (s, 1H), 6.08 (s, 1H), 5.99 (s, 1H), 4.96 (s, 2H), 3.71 (s, 3H).

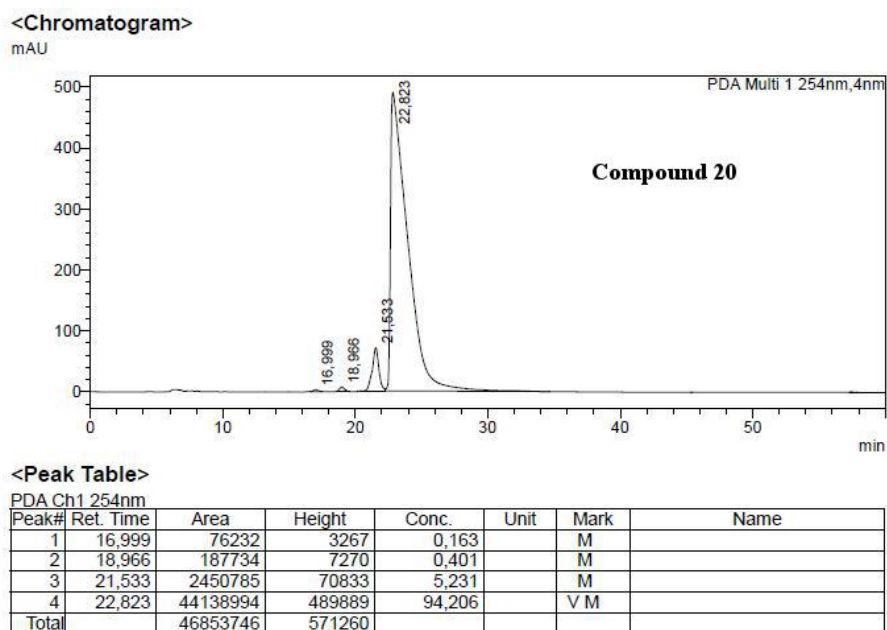
$^{13}\text{C}$  NMR (101 MHz,  $\text{CDCl}_3$ ):  $\delta$ = 161.45, 148.51, 138.73, 137.90, 129.76, 119.83, 106.53, 103.39, 100.49, 55.41, 51.07.

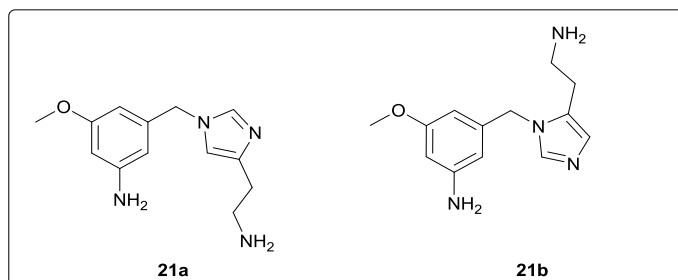
HR-MS (ESI) calcd for  $\text{C}_{11}\text{H}_{14}\text{N}_3\text{O}[\text{M}+\text{H}]^+$  : 204.1131, found: 204.1130.

IR ( $\text{cm}^{-1}$ ): 3345.52, 3214.19, 2924.75, 2852, 1507.71, 1472.39, 1357.93, 1284.14, 1229.8, 1171.95, 1107.2, 1077.48, 1057.06, 913.47, 834.79, 749.31, 687.9, 663.8

Mp = 111–115 °C.

Purity by HPLC > 94%





**3-((4-(Aminomethyl)-1*H*-imidazol-1-yl)methyl)-5-methoxyaniline (**21a**)**

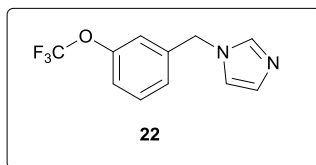
**3-((5-(2-Aminoethyl)-1*H*-imidazol-1-yl)methyl)-5-methoxyaniline (**21b**)**

The mixture of **21a** and **21b** was synthesised according to GP2, starting from **47a** and **47b** (11.4 mg, 0.022 mmol) and  $\text{N}_2\text{H}_4 \cdot \text{H}_2\text{O}$  (50–60 % solution, 39  $\mu\text{L}$ , 0.372 mmol) in MeOH (1.3 mL). Purification by CC( $\text{SiO}_2$ ;  $\text{CH}_2\text{Cl}_2/\text{MeOH}$ , 87:13 to  $\text{CHCl}_3/\text{MeOH}/\text{NH}_3$ , 2:1.5:0.7) afforded the mixture of the two regioisomers **21a** and **21b** as a yellow solid (15mg, 17% over two steps, 1:0.3 ratio, **21a:21b**).

$^1\text{H}$  NMR (400 MHz,  $\text{CD}_3\text{OD}$ ):  $\delta$ =7.66 (s, 1H, **21b**), 7.63 (s, 1H, **21a**), 6.88 (s, 1H, **21a**), 6.81 (s, 1H, **21b**), 6.24 (s, 1H, **21a**), 6.21 (s, 1H, **21b**), 6.17 (s, 1H, **21a**), 6.13 (s, 1H, **21a**), 6.02 (s, 1H, **21b**), 6.00 (s, 1H, **21b**), 5.05 (s, 2H, **21b**), 4.97 (s, 2H, **21a**), 3.70 (s, 3H, **21a**), 3.69 (s, 3H, **21b**), 2.93 (t, 2H, **21a**), 2.76–2.65 (m, 2H, **21a** + 4H, **21b**).

$^{13}\text{C}$  NMR (101 MHz,  $\text{CD}_3\text{OD}$ ):  $\delta$ = 168.83, 162.73, 151.17, 151.02, 140.33, 140.24, 140.16, 139.39, 138.58, 127.05, 118.25, 108.24, 107.19, 104.21, 103.24, 101.46, 101.21, 101.17, 55.67, 55.64, 51.99 (2C), 42.09, 41.34, 31.11, 28.02.

HR-MS (ESI) calcd for  $\text{C}_{13}\text{H}_{19}\text{N}_4\text{O}[M+\text{H}]^+$  : 247.1553, found : 247.1553.



### 1-(3-(Trifluoromethoxy)benzyl)-1H-imidazole (**22**)

**22** was synthesised according to GP1, starting from 1-(bromomethyl)-3-(trifluoromethoxy)benzene (**48**, 95  $\mu$ L, 0.59 mmol) and imidazole (**27**, 40 mg, 0.59 mmol) in anhydrous DMF (3.0 mL). The mixture was stirred at room temperature for 16 h and concentrated *in vacuo*. Purification by CC (SiO<sub>2</sub>; EtOAc/pentane, 4:1) afforded **22** as a transparent oil (85.5 mg, 63%).

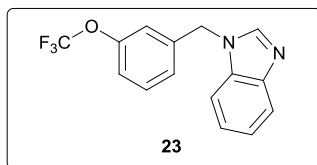
<sup>1</sup>H NMR (400 MHz, CDCl<sub>3</sub>):  $\delta$ =7.59 (s, 1H), 7.37 (t, 1H,  $J$ = 8.0 Hz), 7.17 (d, 1H,  $J$ = 8.2), 7.11 (s, 1H), 7.04 (d, 1H,  $J$ = 7.7 Hz), 6.98 (s, 1H), 6.89 (s, 1H), 5.14 (s, 2H).

<sup>13</sup>C NMR (101 MHz, CDCl<sub>3</sub>):  $\delta$ =149.90, 138.68, 137.62, 130.72, 130.13, 125.57, 121.83, 120.86, 119.93, 119.45, 50.36.

HR-MS (ESI) calcd for C<sub>11</sub>H<sub>10</sub>F<sub>3</sub>N<sub>2</sub>O [ $M+H$ ]<sup>+</sup>: 243.0740, found: 243.0733.

IR (cm<sup>-1</sup>): 1592.19, 1505.9, 1448.57, 1252.5, 1211.04, 1156.32, 1107.38, 1076.09, 1030.06, 1003.01, 906.5, 864.91, 799.71, 736.56, 701.16, 661.99, 629.32.





### 1-(3-(Trifluoromethoxy)benzyl)-1H-benzo[d]imidazole (**23**)

Compound **23** was synthesised according to GP1, starting from 1-(bromomethyl)-3-(trifluoromethoxy)benzene (**48**, 55  $\mu\text{L}$ , 0.34 mmol) and benzimidazole (**49**, 40 mg, 0.34 mmol) in anhydrous DMF (2.3 mL). The mixture was stirred at room temperature for 16 h and concentrated *in vacuo*. Purification by CC (SiO<sub>2</sub>; EtOAc/pentane, 4:1) afforded **23** as a white solid (53 mg, 54%).

<sup>1</sup>H NMR (400 MHz, CD<sub>3</sub>OD):  $\delta$ =8.34 (s, 1H), 7.72–7.70 (m, 1H), 7.45–7.41 (m, 2H), 7.31–7.36 (m, 1H), 7.23 (s, 1H), 7.23–7.19 (m, 3H), 5.57 (s, 2H).

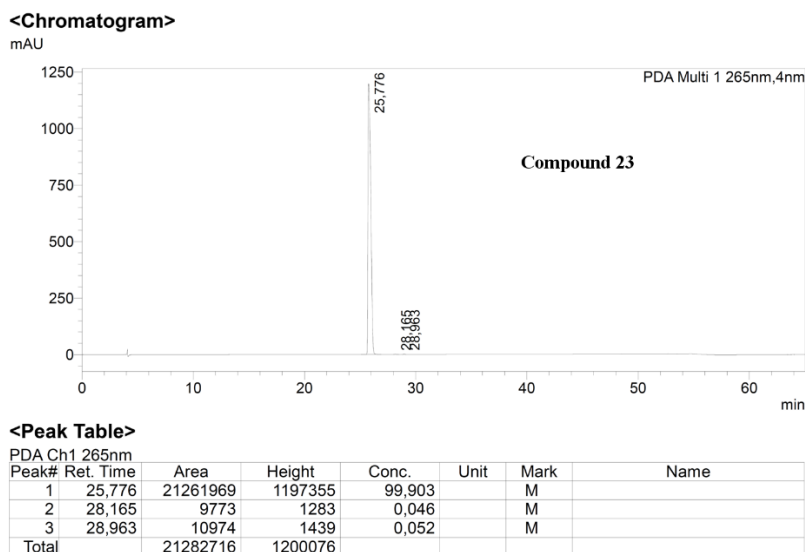
<sup>13</sup>C NMR (101 MHz, CD<sub>3</sub>OD):  $\delta$ =151.03, 145.10, 144.12, 140.54, 131.90, 127.12, 124.77, 124.05, 123.25, 121.69, 121.10, 120.71, 120.35, 111.91, 49.03.

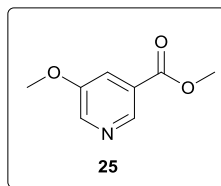
HR-MS (ESI) calcd for C<sub>15</sub>H<sub>12</sub>F<sub>3</sub>N<sub>2</sub>O [*M*+H]<sup>+</sup>: 293.0896, found: 293.0898.

IR (cm<sup>-1</sup>): 3088.93, 1614.62, 1591.79, 1483.87, 1459.00, 1445.01, 1382.76, 1366.02, 1092.02, 1007.82, 984.35, 947.32, 926.19, 886.83, 869.77, 808.33, 778.08, 703.3, 634.13, 616.17, 582.07, 573.9, 533.56, 470.79.

Mp = 45–47 °C.

Purity by HPLC > 99%.





### Methyl 5-methoxynicotinate (**25**)

A round-bottomed flask was charged with **24** (0.6 g, 4.3 mmol, 1.0 eq) and toluene/MeOH (4:1, 175 mL). Trimethylsilyldiazomethane (2 M in Et<sub>2</sub>O, 8.6 mL, 4.0 eq.) was added, and the mixture was allowed to stir at room temperature for 16 h. The solvent was removed *in vacuo*, and the crude mixture was purified by CC (SiO<sub>2</sub>; EtOAc/toluene, 1:4) to afford **25** as a beige solid (719 mg, quant.). Spectral data are consistent with those reported in the literature literature.<sup>[21]</sup>

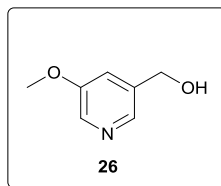
<sup>1</sup>H NMR (400 MHz, CDCl<sub>3</sub>): δ=8.76 (d, 1H, *J*=1.6 Hz), 8.41 (d, 1H, *J*=2.9 Hz), 7.70 (dd, 1H, *J*<sub>1</sub>=2.9 Hz, *J*<sub>2</sub>=1.6 Hz), 3.89 (s, 3H), 3.84 (s, 3H).

<sup>13</sup>C NMR (101 MHz, CDCl<sub>3</sub>): δ= 164.76, 155.16, 141.42, 140.73, 126.21, 120.34, 55.36, 52.00.

m.p. = 61–63 °C.

HR-MS (ESI) calcd for C<sub>8</sub>H<sub>10</sub>NO<sub>3</sub> [*M*+H]<sup>+</sup>: 168.0662, found: 168.0655.

IR: 2923.37, 2472.67, 1726.25, 1579.98, 1504.52, 1454.67, 1433.96, 1389.30, 1310.24, 1236.98, 1158.85, 1105.33, 1024.03, 995.57, 873.73, 801.57, 764.56, 728.28, 690.10.



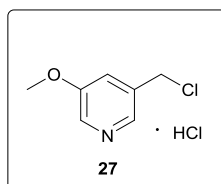
### (5-Methoxypyridin-3-yl)methanol (**26**)

A dry flask under was charged with **25** (30 mg, 0.18 mmol, 1.0 eq.) and CH<sub>2</sub>Cl<sub>2</sub> (1.0 mL). The mixture was cooled down to -78 °C, and DIBAL-*H* (1 M in CH<sub>2</sub>Cl<sub>2</sub>, 0.6 mL, 0.57 mmol, 3.2 eq.) was added. The mixture was allowed to stir at 0 °C for 16 h, then quenched with a sat. aq. sodium tartrate solution (1.0 mL). The mixture was diluted with CH<sub>2</sub>Cl<sub>2</sub> (5.0 mL) and stirred for 1 h. The layers were separated, and the aqueous phase was washed with CH<sub>2</sub>Cl<sub>2</sub> (3 x 5.0 mL). The organic layers were dried over MgSO<sub>4</sub>, filtered and concentrated *in vacuo* to afford **26** as a yellow oil (24.2 mg, 97%).

<sup>1</sup>H NMR (400 MHz, CDCl<sub>3</sub>): δ=8.12 (s, 1H), 8.07 (s, 1H), 7.25 (s, 1H), 4.67 (s, 2H), 3.82 (s, 3H).

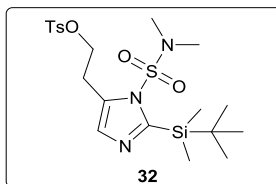
<sup>13</sup>C NMR (101 MHz, CD<sub>3</sub>OD): δ= 157.95, 140.82, 140.24, 136.98, 120.95, 62.47, 56.34.

HR-MS (ESI) calcd for C<sub>7</sub>H<sub>10</sub>NO<sub>2</sub> [*M*+H]<sup>+</sup>: 140.0706, found: 140.0697.



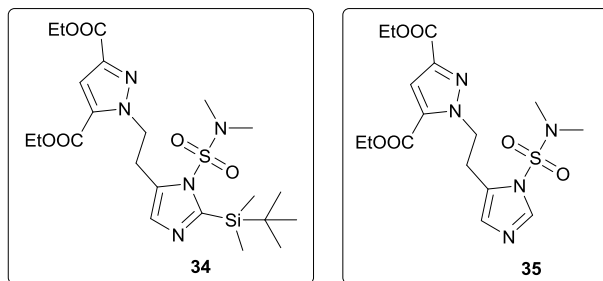
### 3-(Chloromethyl)-5-methoxypyridine hydrochloride (**27**)

A dry flask was charged with **26** (37 mg, 0.27 mmol, 1.0 eq.) and CHCl<sub>3</sub> (3.0 mL). SOCl<sub>2</sub> (21.0 μL, 0.29 mmol, 1.1 eq.) was added, and the mixture was stirred at room temperature for 45 minutes. The solvent was removed *in vacuo* to afford a brown solid. The product was used for the next step without any further purification.



**2-(2-(*Tert*-butyldimethylsilyl)-1-(*N,N*-dimethylsulfamoyl)-1*H*-imidazol-5-yl)ethyl 4-methylbenzenesulfonate (32)**

To a solution of **31** (50.0 mg, 0.15 mmol, 1.0 eq.) in CH<sub>2</sub>Cl<sub>2</sub> (1.4 mL), cetrimonium bromide (3.0 mg, 0.01 mmol, 0.05 eq.) and an aq. solution of NaOH (50%, 0.2 mL) were added. After that, a solution of *p*-toluenesulfonyl chloride (35 mg, 0.18 mmol, 1.2 eq.) in CH<sub>2</sub>Cl<sub>2</sub> (0.2 mL) was added, and the mixture was allowed to stir at room temperature for 16 h. The layers were separated, and the organic phase was washed with H<sub>2</sub>O (3 x 1.0 mL) and a sat. aq. NaCl solution (1 x 1.0 mL), dried over MgSO<sub>4</sub>, filtered and concentrated *in vacuo*. The product was used in the next step without further purification.



**Diethyl 1-(2-(2-(*tert*-butyldimethylsilyl)-1-(*N,N*-dimethylsulfamoyl)-1*H*-imidazol-5-yl)ethyl)-1*H*-pyrazole-3,5-dicarboxylate (34)**

**Diethyl 1-(2-(1-(*N,N*-dimethylsulfamoyl)-1*H*-imidazol-5-yl)ethyl)-1*H*-pyrazole-3,5-dicarboxylate (35)**

A dry flask was charged with diethyl *1H*-pyrazole-3,5-dicarboxylate (**33**) (3.18 mg, 15.0 mmol, 2.0 eq.) in anhydrous DMF (50 mL). NaH (60% dispersion in mineral oil, 0.57 g, 14.3 mmol, 1.9 eq.) was added, and the suspension was stirred at room temperature for 30 minutes. A solution of **32** (3.66 g, 7.5 mmol, 1.0 eq.) in DMF (50 mL) was added dropwise, and the mixture was stirred at room temperature for 16 h. After quenching with a sat. aq. NaCl solution (10 mL), the crude was extracted with Et<sub>2</sub>O (3 x 10 mL) and concentrated *in vacuo*. Purification by CC (SiO<sub>2</sub>; EtOAc/toluene, 1:5) afforded **34** as a colourless oil (2.20 g, 56%).

<sup>1</sup>H NMR (400 MHz, CDCl<sub>3</sub>): δ=7.28 (s, 1H), 6.75 (s, 1H), 4.90 (t, 2H, *J*=7.1 Hz), 4.38 (q, 2H, *J*=7.1 Hz), 4.27 (q, 2H, *J*=7.0 Hz), 3.35 (t, 2H, *J*=7.0 Hz), 2.80 (s, 6H), 1.34 (m, 6H), 0.95 (s, 9H), 0.33 (s, 6H).

<sup>13</sup>C NMR (101 MHz, CDCl<sub>3</sub>): δ=161.63, 159.08, 155.97, 142.69, 134.11, 130.46, 130.33, 114.13, 61.69, 61.38, 50.75, 37.88 (2C), 27.37 (3C), 26.10, 18.54, 14.51, 14.30, -3.52 (2C).

HR-MS (ESI) calcd for C<sub>22</sub>H<sub>38</sub>N<sub>5</sub>O<sub>8</sub>SSi [*M*+*H*]<sup>+</sup>: 528.2307, found: 528.2296.

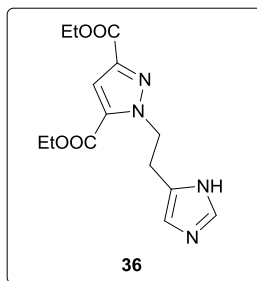
The partially deprotected compound **35** was also isolated as a yellow oil (1.20 g, 20%).

<sup>1</sup>H NMR (400 MHz, CDCl<sub>3</sub>): δ=7.83 (s, 1H), 7.27 (s, 1H), 6.60 (s, 1H), 4.93 (t, 2H, *J*=6.9 Hz), 4.37 (q, 2H, *J*=7.1 Hz), 4.26 (q, 2H, *J*=7.1 Hz), 3.34 (t, 2H, *J*=6.9 Hz), 2.87 (s, 6H), 1.30–1.38 (m, 6H).

<sup>13</sup>C NMR (101 MHz, CDCl<sub>3</sub>): δ=161.64, 159.05, 142.81, 138.71, 136.67, 134.26, 129.70, 128.11, 114.06, 61.75, 61.43, 50.72, 38.24, 26.21, 14.53, 14.32.

HR-MS (ESI) calcd for C<sub>16</sub>H<sub>24</sub>N<sub>5</sub>O<sub>6</sub>S [*M*+*H*]<sup>+</sup>: 414.1442, found: 414.1535.

IR (cm<sup>-1</sup>): 3133.1, 2982.2, 2938.8, 1718.4, 1527.9, 1464.6, 1440.0, 1418.0, 1387.9, 1259.6, 1213.5, 1172.8, 1149.3, 1084.0, 1027.6, 964.0, 904.0, 847.7, 766.1, 726.2, 651.5, 589.3, 515.3.



### Diethyl 1-(2-(1*H*-imidazol-5-yl)ethyl)-1*H*-pyrazole-3,5-dicarboxylate (**36**)

A dry flask was charged with **34** (0.17 g, 0.32 mmol, 1.0 eq.) in HCl (1.25 M in EtOH, 5.8 mL). The mixture was stirred at room temperature for 16 h, and the solvent was removed *in vacuo*. The crude mixture was taken up in EtOAc (5 mL) and washed with a sat. aq. NaHCO<sub>3</sub> solution (3 x 4.0 mL). The organic phase was dried over MgSO<sub>4</sub>, filtered and concentrated *in vacuo* to afford the product as an off-white solid (70 mg, 68%).

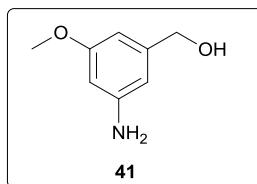
<sup>1</sup>H NMR (400 MHz, CD<sub>3</sub>OD):  $\delta$ =7.57 (s, 1H), 7.23 (s, 1H), 6.70 (s, 1H), 4.85 (t, 2H,  $J$ =7.0 Hz), 4.33 (two overlapping quartets, 4H,  $J$ =7.2 Hz), 3.13 (t, 2H,  $J$ =7.0 Hz), 1.36 (two overlapping triplets, 6H,  $J$ =7.2 Hz).

<sup>13</sup>C NMR (101 MHz, CD<sub>3</sub>OD):  $\delta$  163.11, 160.22, 143.43, 136.36, 135.58, 134.78, 118.40, 114.37, 62.77, 62.37, 53.42, 29.16, 14.70, 14.60.

HR-MS (ESI) calcd for C<sub>14</sub>H<sub>19</sub>N<sub>4</sub>O<sub>4</sub> [ $M+H$ ]<sup>+</sup>: 307.1401, found: 307.1400

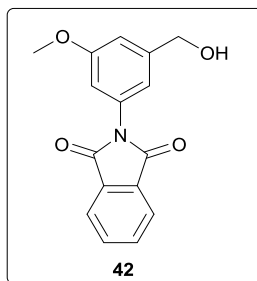
IR: 3336.5, 3128.4, 2984.7, 2873.0, 2638.0, 1721.3, 1577.9, 1528.1, 1471.1, 1447.3, 1383.9, 1366.1, 1333.6, 1302.9, 1261.1, 1211.6, 1166.2, 1099.3, 1088.8, 1058.4, 1026.5, 987.7, 847.7, 815.3, 798.9, 784.8, 721.3, 698.3, 635.2, 584.4.

Mp = 118–119 °C.



**(3-Amino-5-methoxyphenyl)methanol (41)**

LiAlH<sub>4</sub> (273 mg, 7.2 mmol) was added to a dry flask under nitrogen and cooled down to 0 °C, then dry THF (5 mL) was slowly added. A suspension of **40** (800 mg, 4.8 mmol) in dry THF (8 mL) was added dropwise, and the reaction mixture was heated to reflux for 16 h. After cooling to 0 °C, water (0.3 mL), an aq. NaOH solution (15%, 0.3 mL) and water (0.9 mL) were subsequently added, and the mixture was left to stir at room temperature for 1 h. After dilution with CH<sub>2</sub>Cl<sub>2</sub>, the mixture was filtered through Celite and concentrated *in vacuo*. The crude was used in the next step without any further purification.



### 2-(3-(Hydroxymethyl)-5-methoxyphenyl)isoindoline-1,3-dione (**42**)

A mixture of **41** (129 mg, 0.84 mmol), phthalic anhydride (124 mg, 0.84 mmol) and pyridine (4.2 mL) was stirred at 80 °C for 3 h. The reaction mixture was then cooled down, diluted with CH<sub>2</sub>Cl<sub>2</sub> (20 mL) and washed with a sat. aq. CuSO<sub>4</sub> solution until a blue colour appeared in the aqueous phase. The organic phase was washed with water (2 x 10 mL), dried over Na<sub>2</sub>SO<sub>4</sub>, filtered and concentrated *in vacuo*. Purification by CC (SiO<sub>2</sub>; EtOAc/pentane, 2:3) afforded **42** as a white solid (605 mg, 68%).

<sup>1</sup>H NMR (400 MHz, CDCl<sub>3</sub>): δ=7.94–7.92 (m, 2H), 7.79–7.76 (m, 2H), 6.99 (s, 1H), 6.97 (s, 1H), 6.87 (s, 1H), 4.71 (s, 2H), 3.82 (s, 3H).

<sup>13</sup>C NMR (101 MHz, CDCl<sub>3</sub>): δ=167.43 (2C), 160.47, 143.59, 134.66, 132.88 (2C), 131.90 (2C), 124.00, 117.36, 112.43, 111.91, 65.04, 55.75.

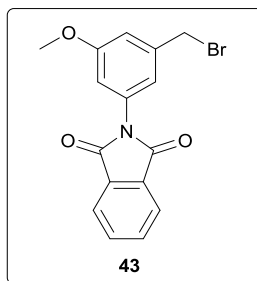
HR-MS (ESI) calcd for C<sub>16</sub>H<sub>14</sub>NO<sub>4</sub> [M+H]<sup>+</sup>: 284.0917, found: 284.0913.

IR (cm<sup>-1</sup>): 1765.56, 1712, 1603.24, 1467.07, 1391.04, 1346.22, 1280.81, 1197.07, 1159.44, 1115.99, 1031.98, 984.83, 954, 921.13, 895.91, 844.2, 794.52, 744.98, 712.38, 685.07, 670.51, 636.9, 530.11.

Mp = 168–171 °C.

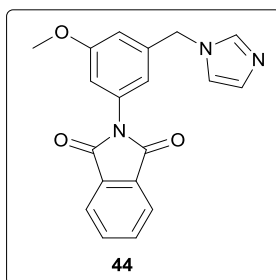
Anal. Calculated for C<sub>16</sub>H<sub>13</sub>NO<sub>4</sub> (283.28): C 67.84, H 4.63, N 4.94; found: C 67.67, H 4.72, N 5.06.





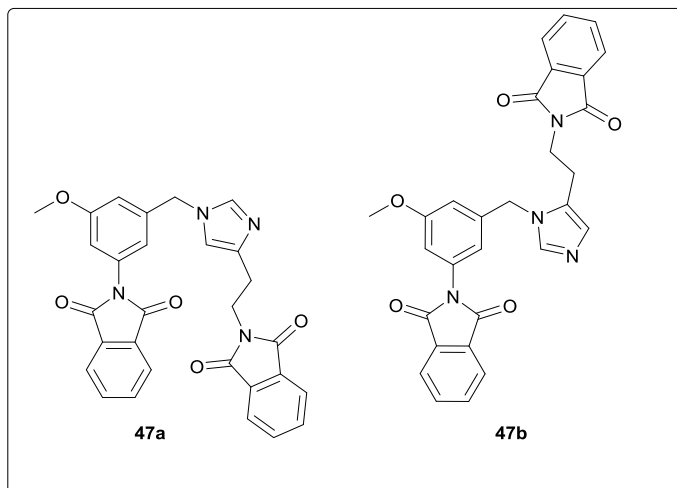
### 2-(3-(Bromomethyl)-5-methoxyphenyl)isoindoline-1,3-dione (**43**)

A solution of **42** (10 mg, 0.035 mmol) in CH<sub>2</sub>Cl<sub>2</sub> (0.8 mL) was treated with SOBr<sub>2</sub> (3.3 μL, 0.042 mmol) and the reaction mixture was left to stir at room temperature. After 1 h, more SOBr<sub>2</sub> (3.3 μL, 0.042 mmol) was added given that the reaction was not complete. After 6 h, more SOBr<sub>2</sub> was added (3.3 μL, 0.042 mmol), and the reaction mixture was left to stir at room temperature for 16 h. After quenching with sat. aq. NH<sub>4</sub>Cl (1 mL), the organic layers were washed with H<sub>2</sub>O (2 x 1.5 mL) and sat. aq. NaCl solution (1 x 1.5 mL), dried over Na<sub>2</sub>SO<sub>4</sub>, filtered and concentrated *in vacuo*. The remaining oil was used in the next step without any further purification.



### 2-(3-((1*H*-Imidazol-1-yl)methyl)-5-methoxyphenyl)isoindoline-1,3-dione (**44**)

Compound **44** was synthesised according to GP1, starting from **43** (11.0 mg, 0.032 mmol) and imidazole (**27**, 2.0 mg, 0.029 mmol) in anhydrous DMF (0.22 mL). The mixture was stirred at room temperature for 16 h and concentrated *in vacuo*. The residue was taken up in CH<sub>2</sub>Cl<sub>2</sub> (2.0 mL) and filtered through Celite. The filter was washed with a mixture of CH<sub>2</sub>Cl<sub>2</sub>/MeOH (95:5) and the second filtrate was concentrated *in vacuo* to afford a crude product, which was used in the next step without any further purification.



**2-(2-(1-(3-(1,3-Dioxoisoindolin-2-yl)-5-methoxybenzyl)-1H-imidazol-4-yl)ethyl)isoindoline-1,3-dione (47a)**

**2-(2-(1-(3-(1,3-Dioxoisoindolin-2-yl)-5-methoxybenzyl)-1H-imidazol-5-yl)ethyl)isoindoline-1,3-dione (47b)**

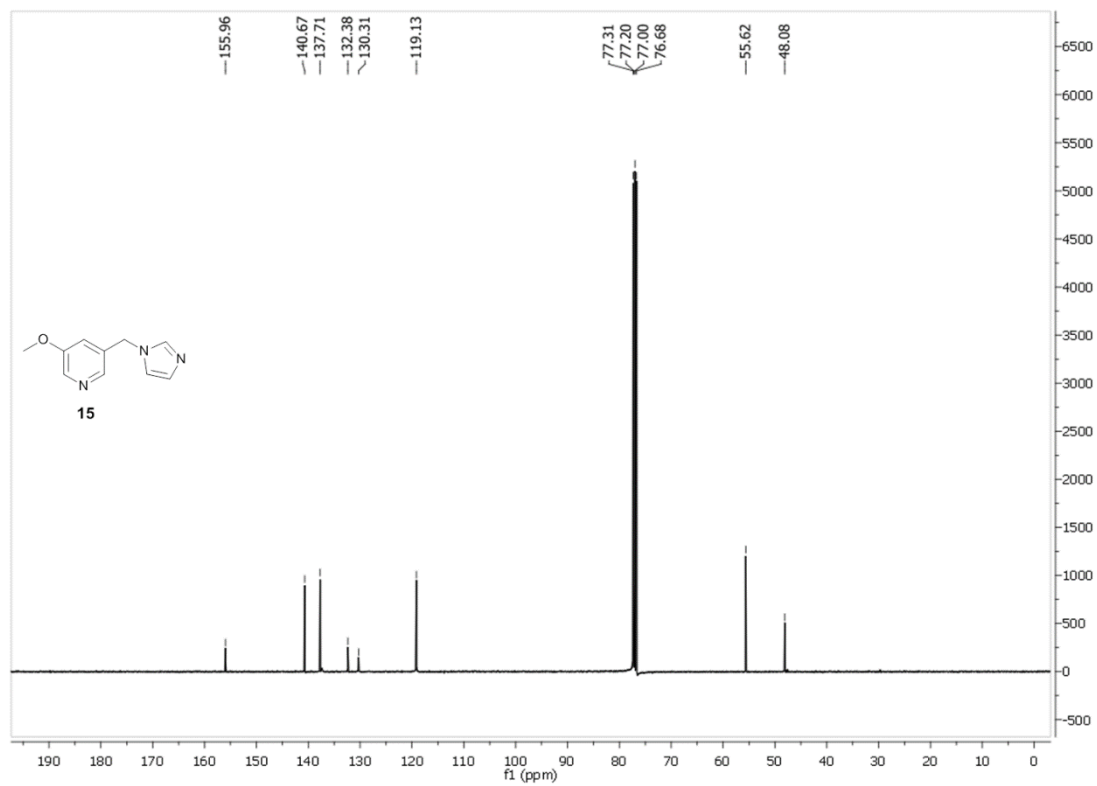
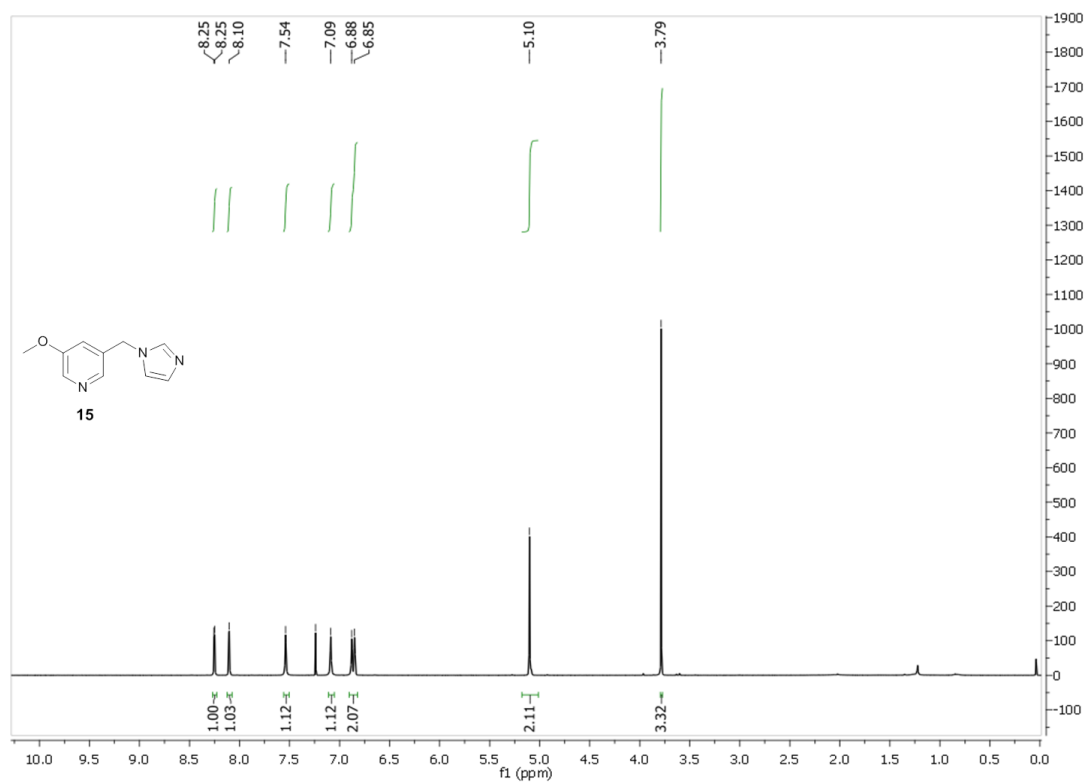
**47a** and **47b** were synthesised according to GP1, starting from **43** (135.7 mg, 0.39 mmol) and **46** (86 mg, 0.36 mmol) in anhydrous DMF (2.4 mL). The mixture was stirred at room temperature for 16 h and concentrated *in vacuo*. The residue was taken up in CH<sub>2</sub>Cl<sub>2</sub> (4.0 mL) and filtered through Celite. The filter was washed with a mixture of CH<sub>2</sub>Cl<sub>2</sub>/MeOH (95:5) and the second filtrate was concentrated *in vacuo* to afford a crude mixture of **47a** and **47b** (ratio 1 : 0.2), which was used in the next step without any further purification. The formation of the products was confirmed by <sup>1</sup>H-NMR, <sup>13</sup>C-NMR and HR-MS.

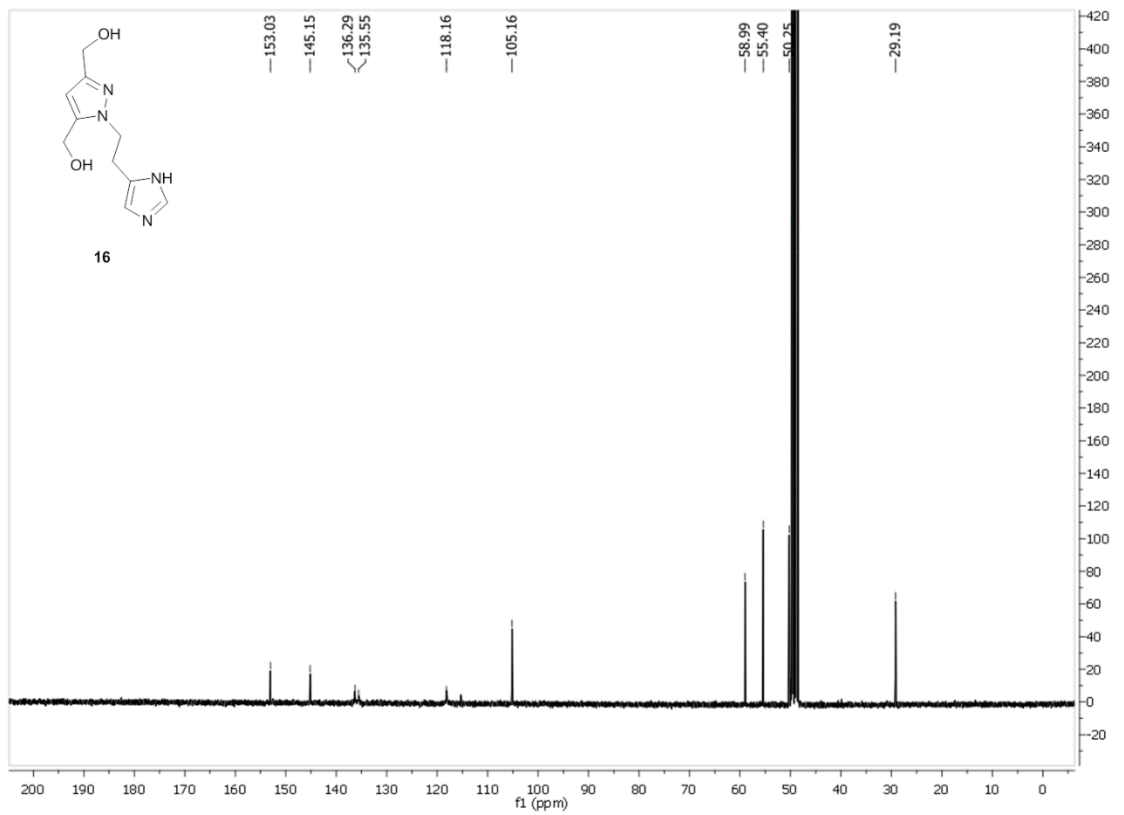
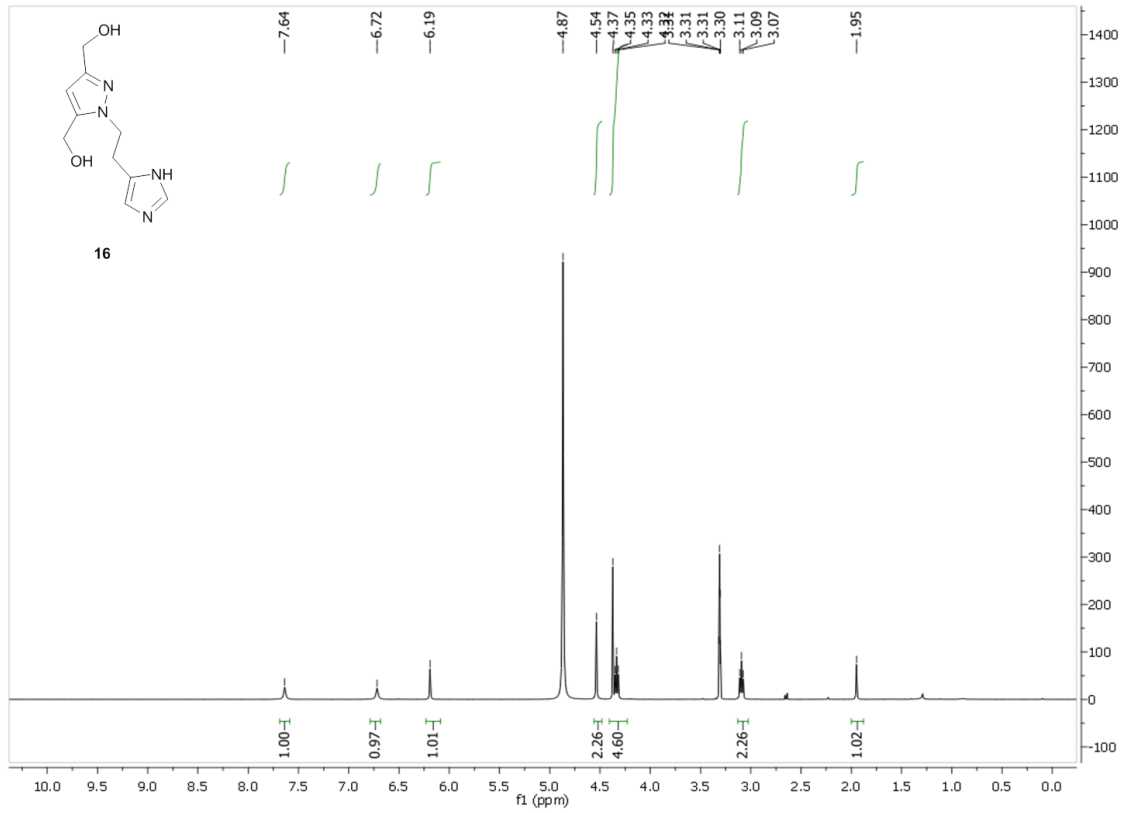
<sup>1</sup>H NMR (400 MHz, CDCl<sub>3</sub>): δ= 7.91–7.62 (m, 8H, **47a**; m, 8H+1H, **47b**) 7.51 (s, 1H) 6.90 (s, 1H, **47a**; s, 1H **47b**), 6.79 (s, 1H **47a**), 6.77 (s, 1H, **47b**), 6.70 (s, 1H, **47a**), 6.65 (s, 1H, **47b**), 6.62 (s, 1H, **47a**), 5.22 (s, 2H, **47b**), 5.03 (s, 2H, **47a**), 3.91 (t, 2H, *J*=7.1 Hz, **47a**), 3.80 (t, 2H, *J*=7.4 Hz, **47b**), 3.76 (s, 3H, **47a**), 3.75 (s, 3H, **47b**), 2.93–2.87 (m, 2H, **47a**; 2H, **47b**),

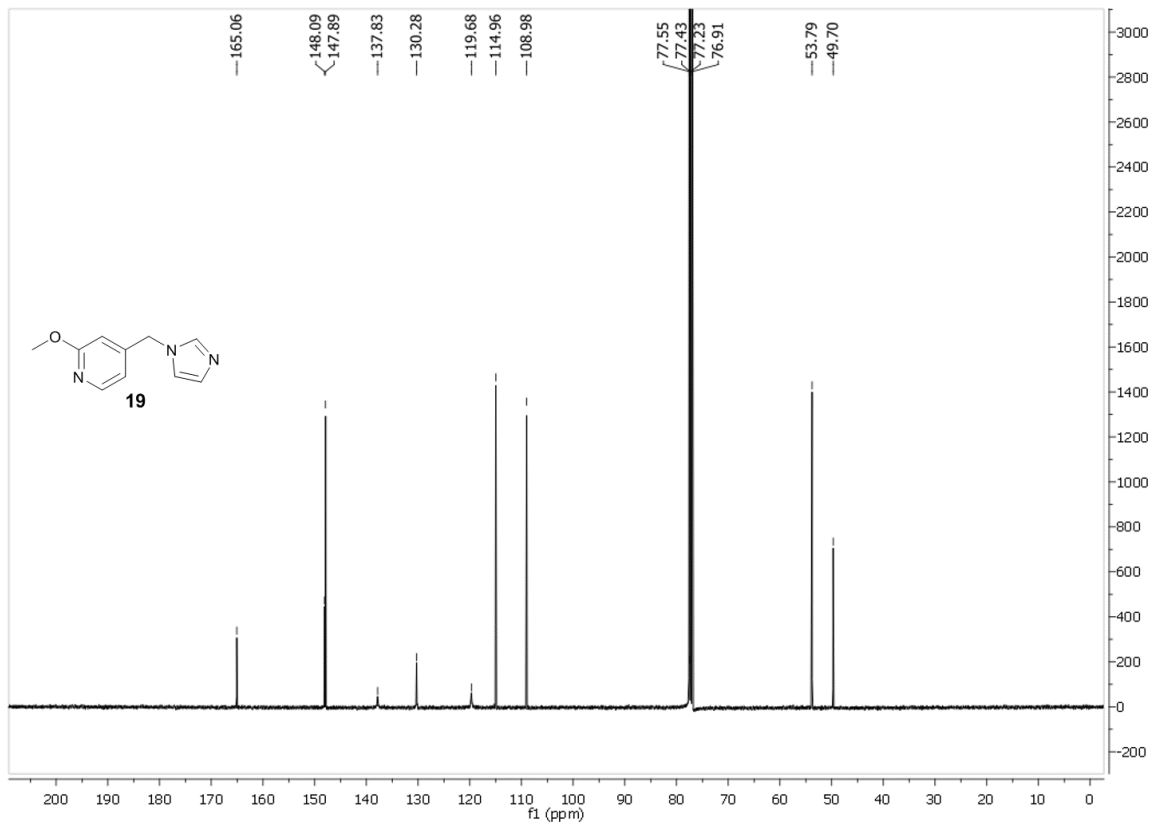
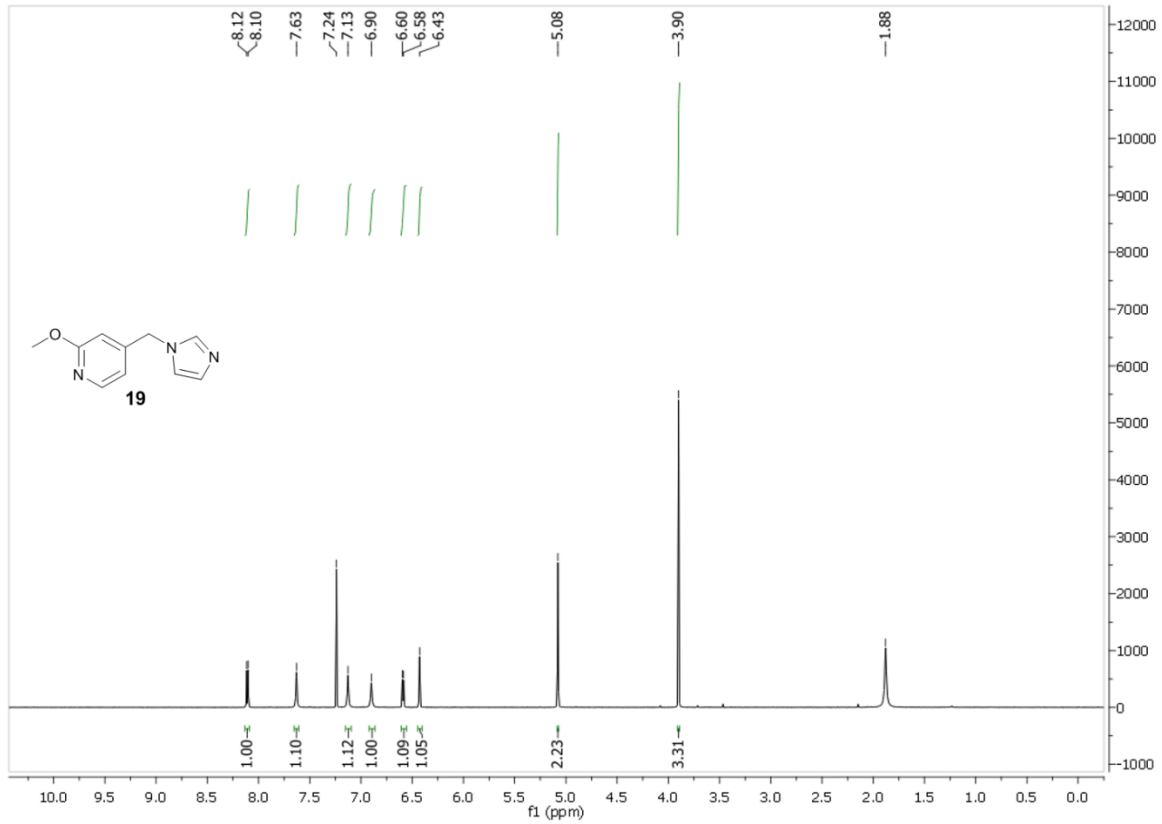
<sup>13</sup>C NMR (400 MHz, CDCl<sub>3</sub>): δ=168.35 (2C, **47a**), 168.19 (2C, **47b**), 167.19 (2C, **47a**), 167.11 (2C, **47b**), 160.76 (**47b**), 160.64 (**47a**), 139.44 (**47b**), 138.45 (**47a**), 138.10 (**47b**), 137.13 (**47a**), 134.71 (4C, **47a**), 134.68 (4C,**47b**), 134.19 (4C, **47b**), 133.94 (4C, **47a**), 133.50 (**47b**), 133.37 (**47a**), 132.23 (**47a**), 132.02 (**47b**), 131.72 (**47a**, **47b**), 123.97 (2C, **47a**), 123.94 (2C, **47b**), 123.48 (2C, **47b**), 123.30 (2C, **47a**), 117.62 (**47a**), 117.31 (**47b**), 112.85 (**47a**), 112.40 (**47b**), 112.17 (**47b**), 112.11 (**47a**), 55.74 (**47a**, **47b**), 50.73 (**47a**), 50.69 (**47b**), 38.00 (**47a**), 36.73 (**47b**), 29.82 (**47b**), 27.34 (**47a**).

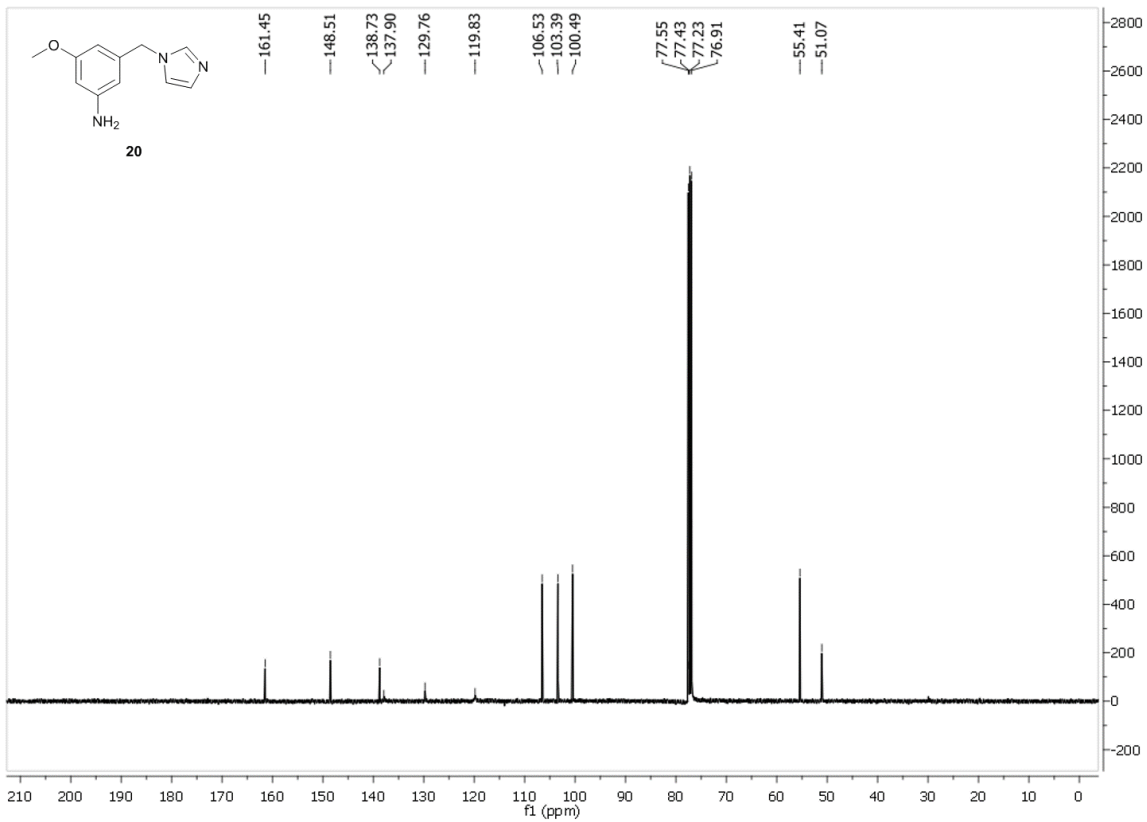
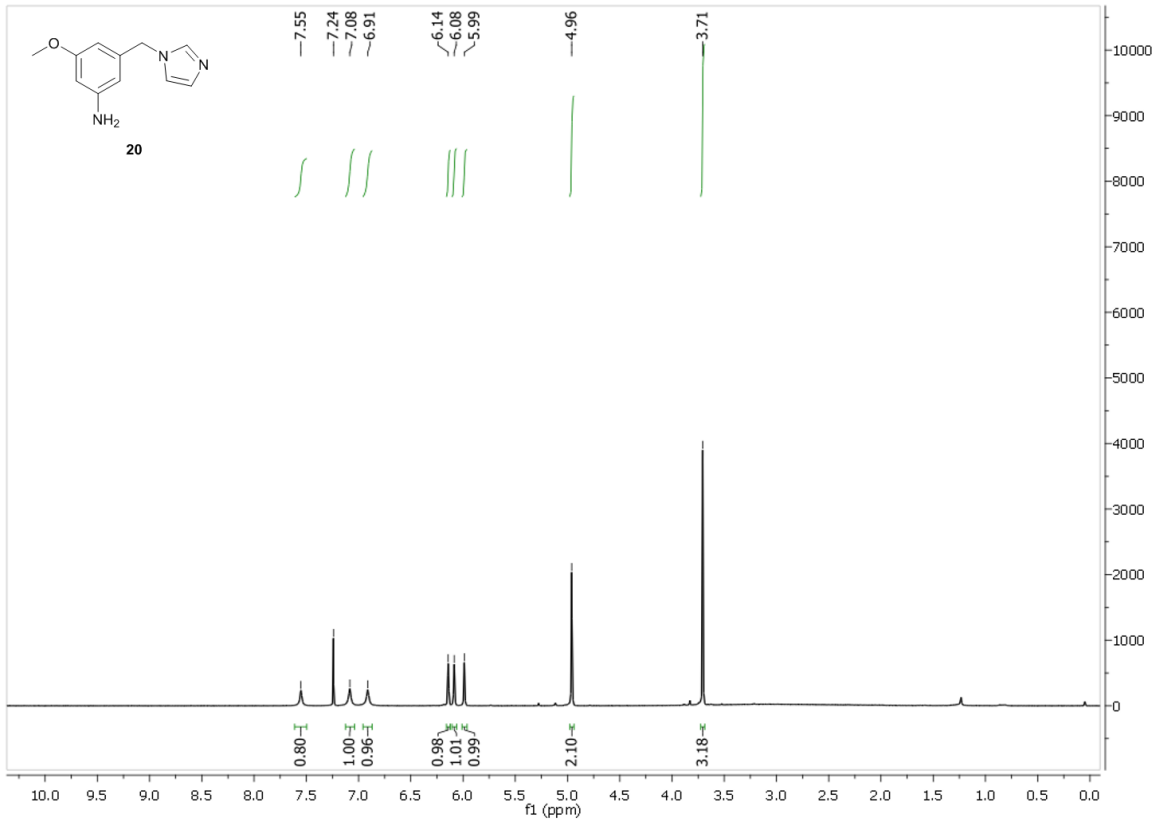
HR-MS (ESI) calcd for C<sub>29</sub>H<sub>22</sub>N<sub>4</sub>O<sub>5</sub> [*M*+H]<sup>+</sup>: 507.16630, found: 506.16582

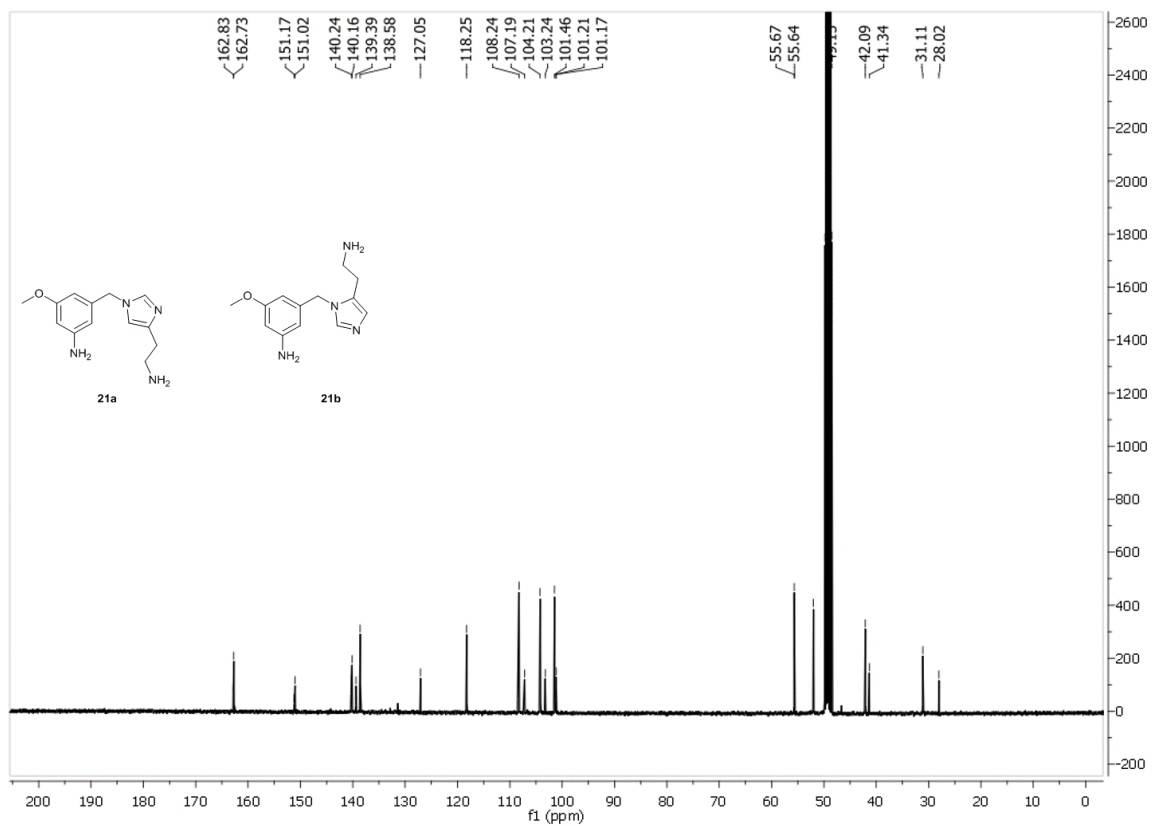
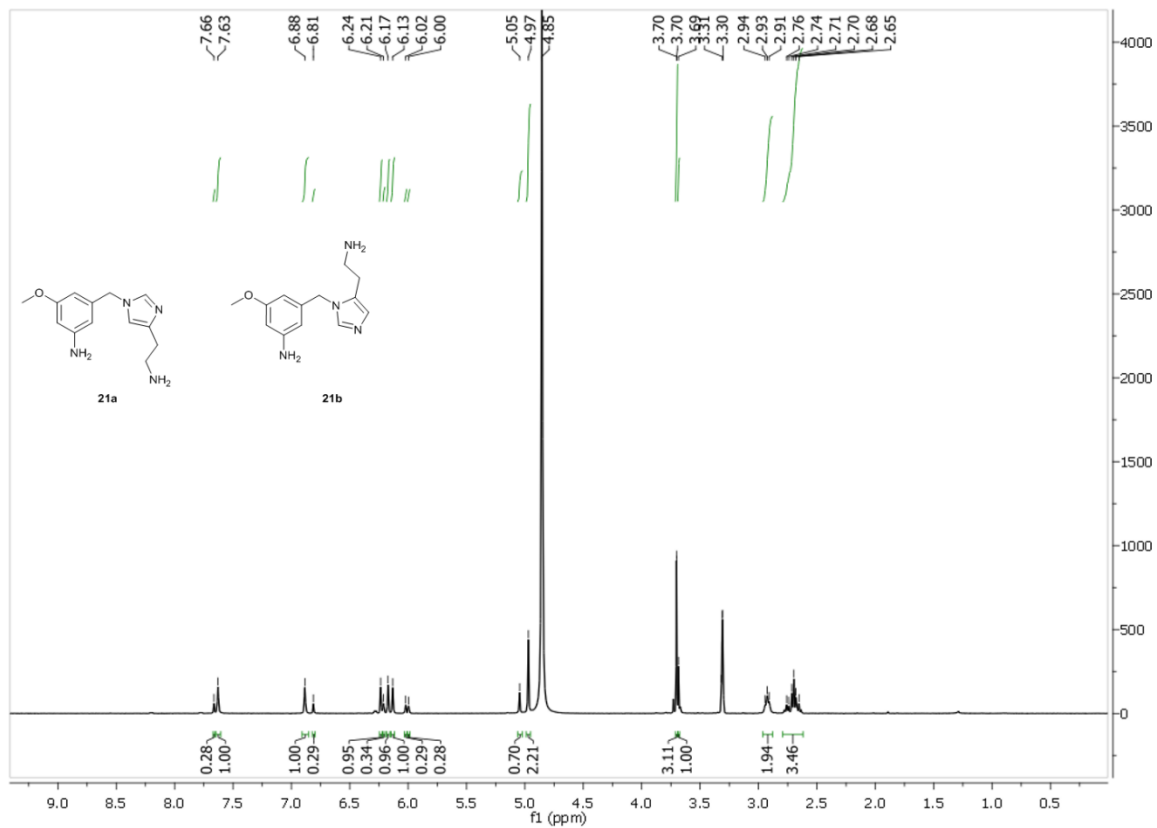
## NMR spectra of the described compounds

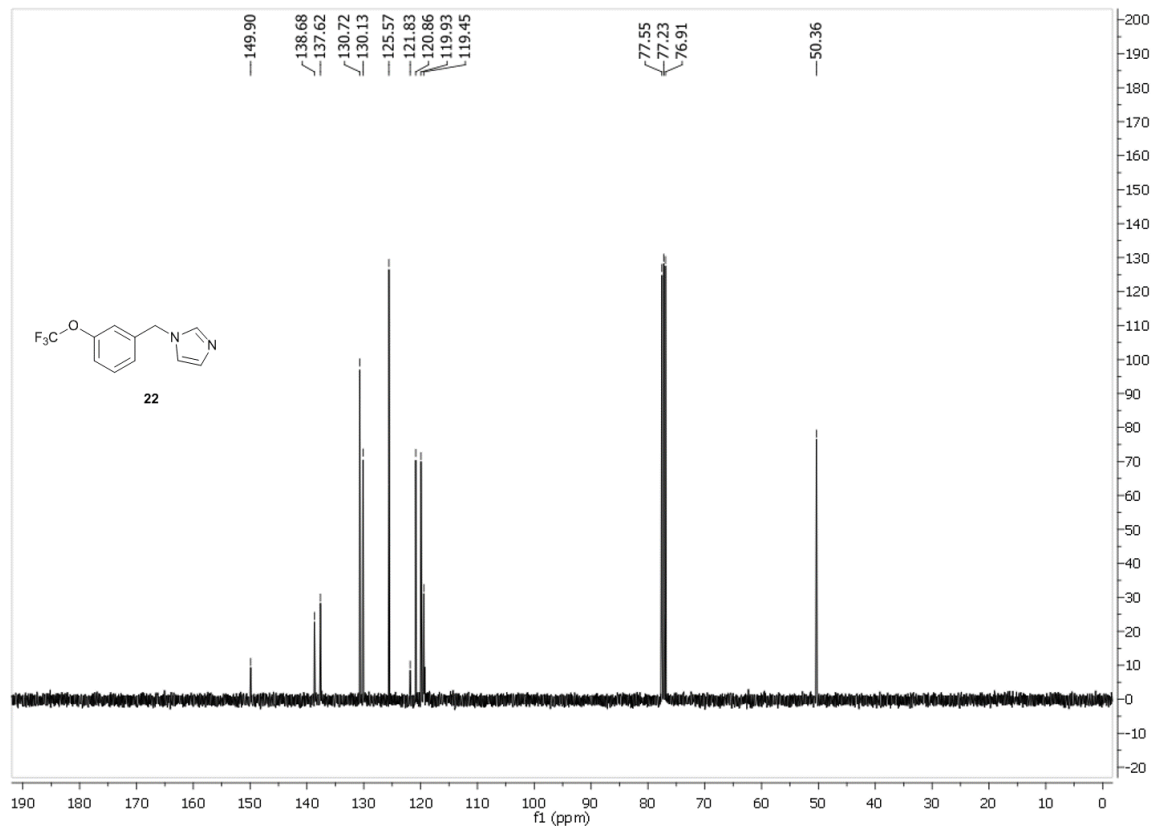
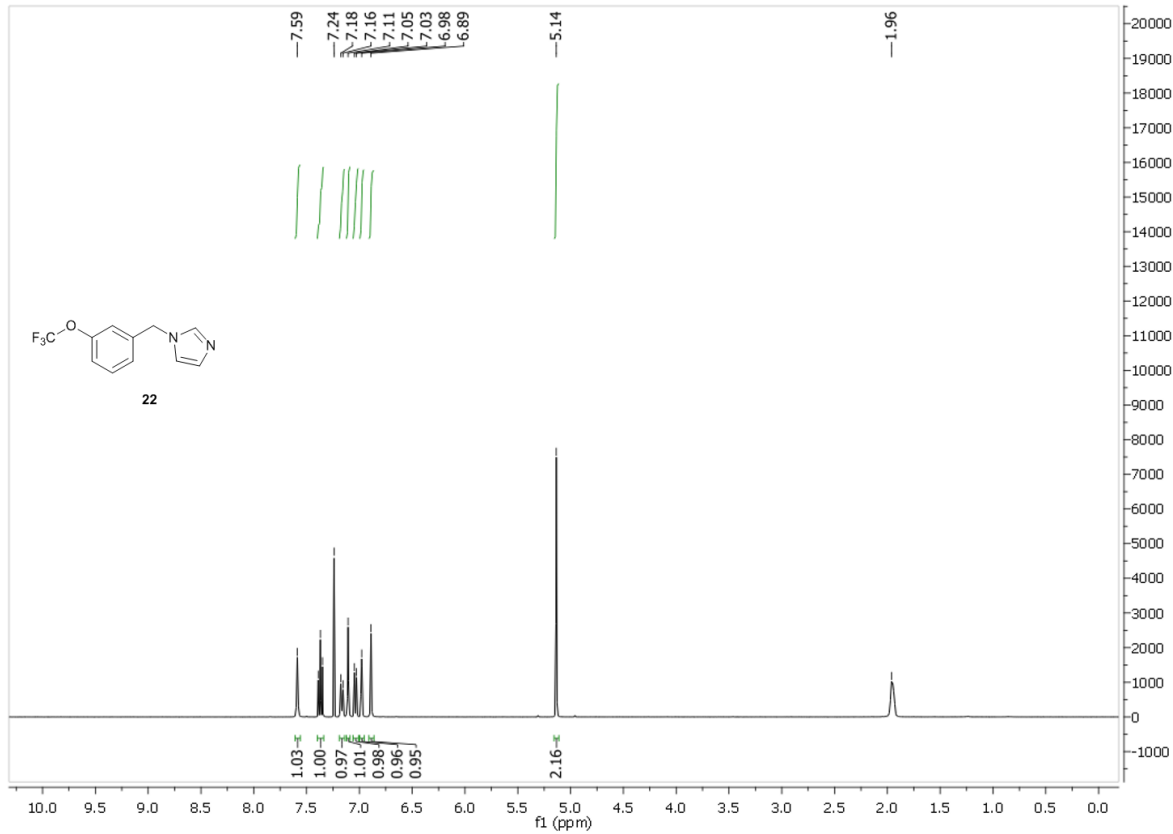




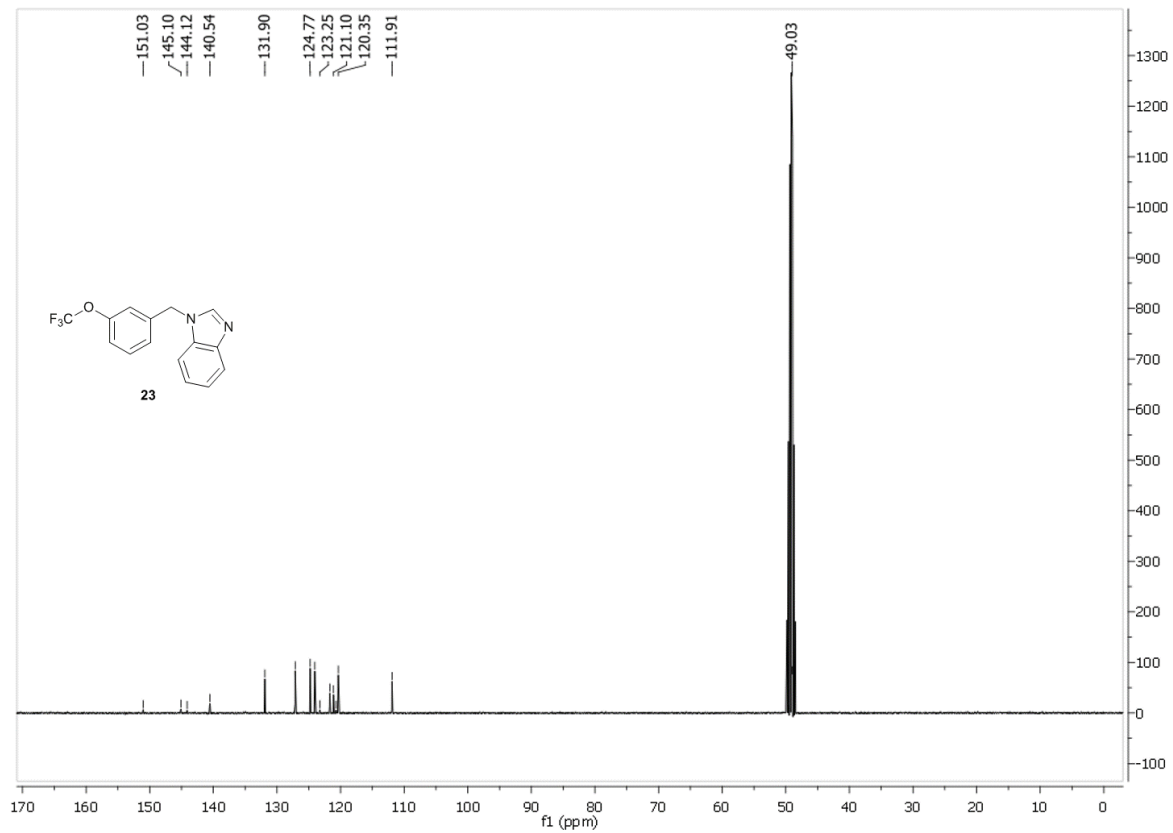
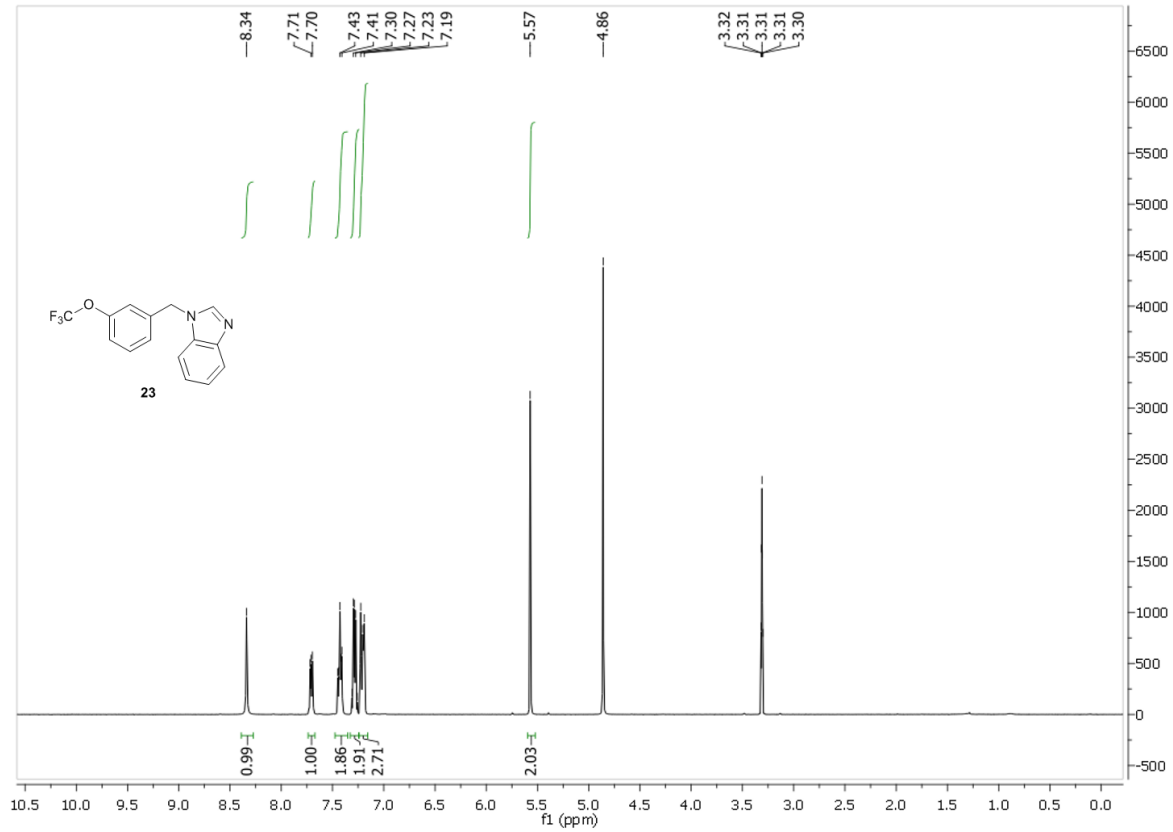


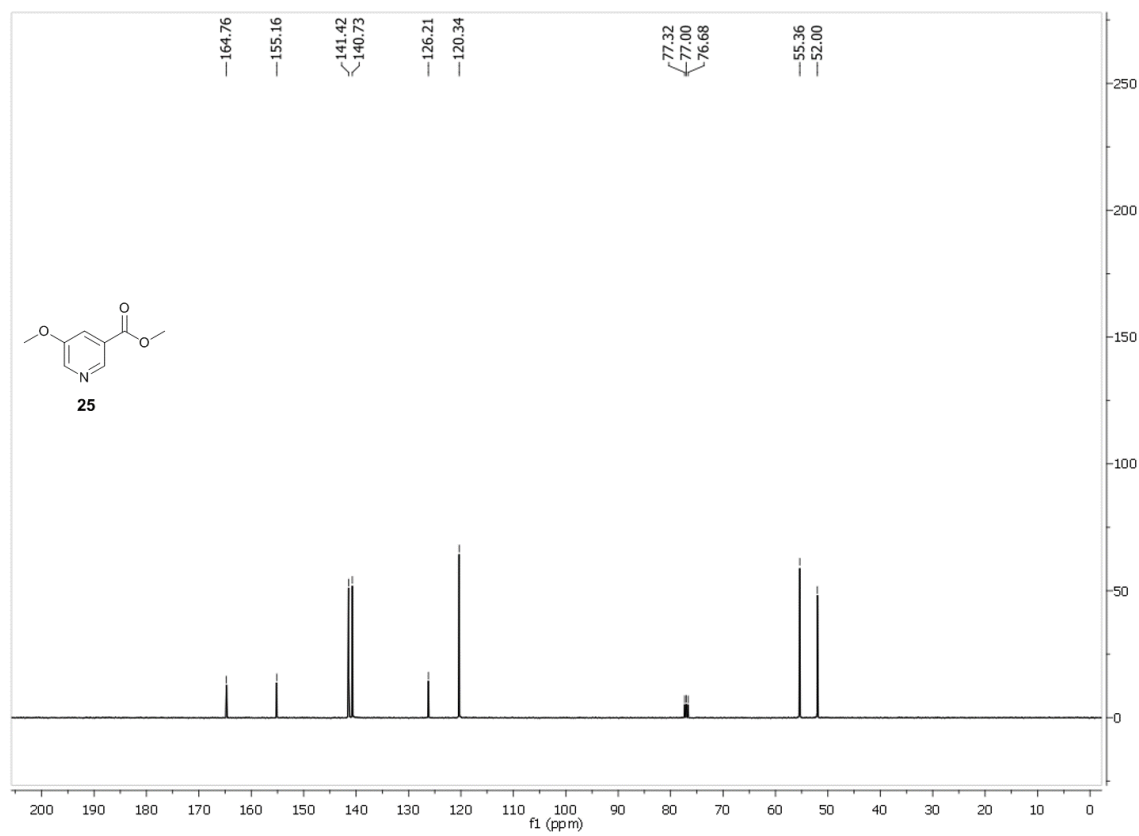
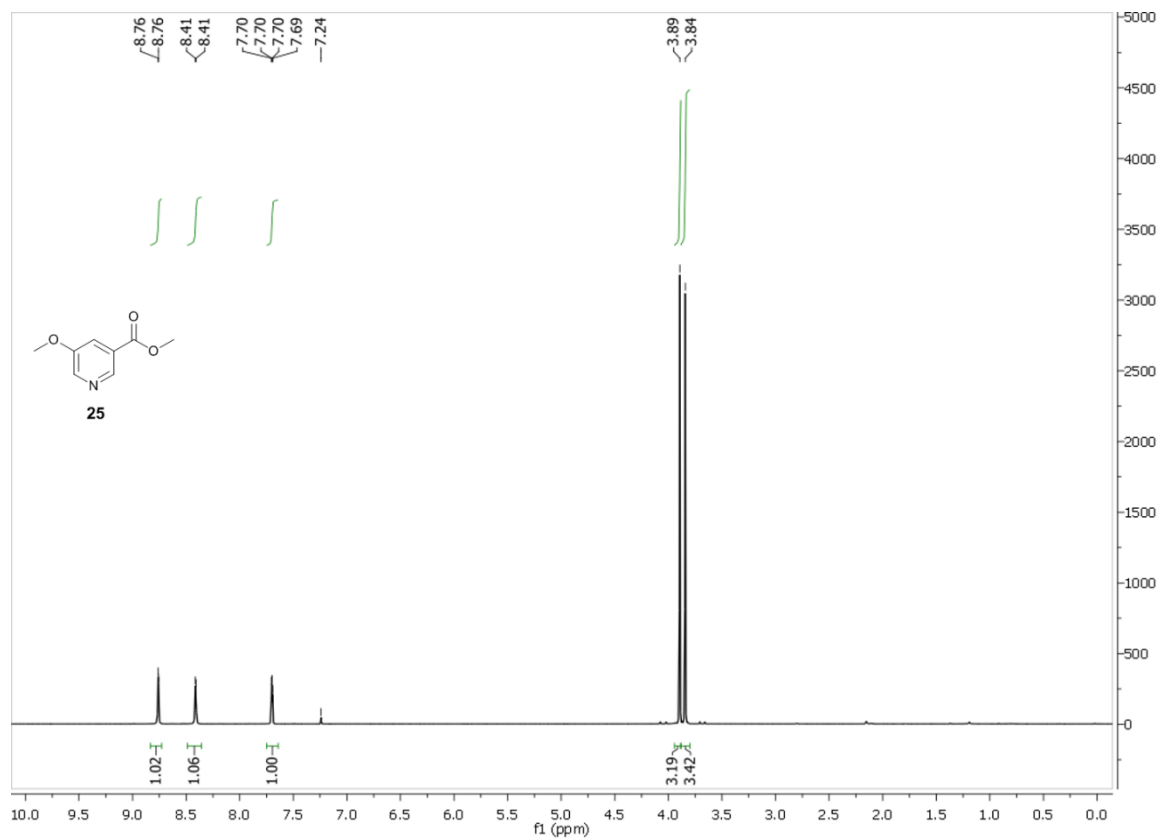


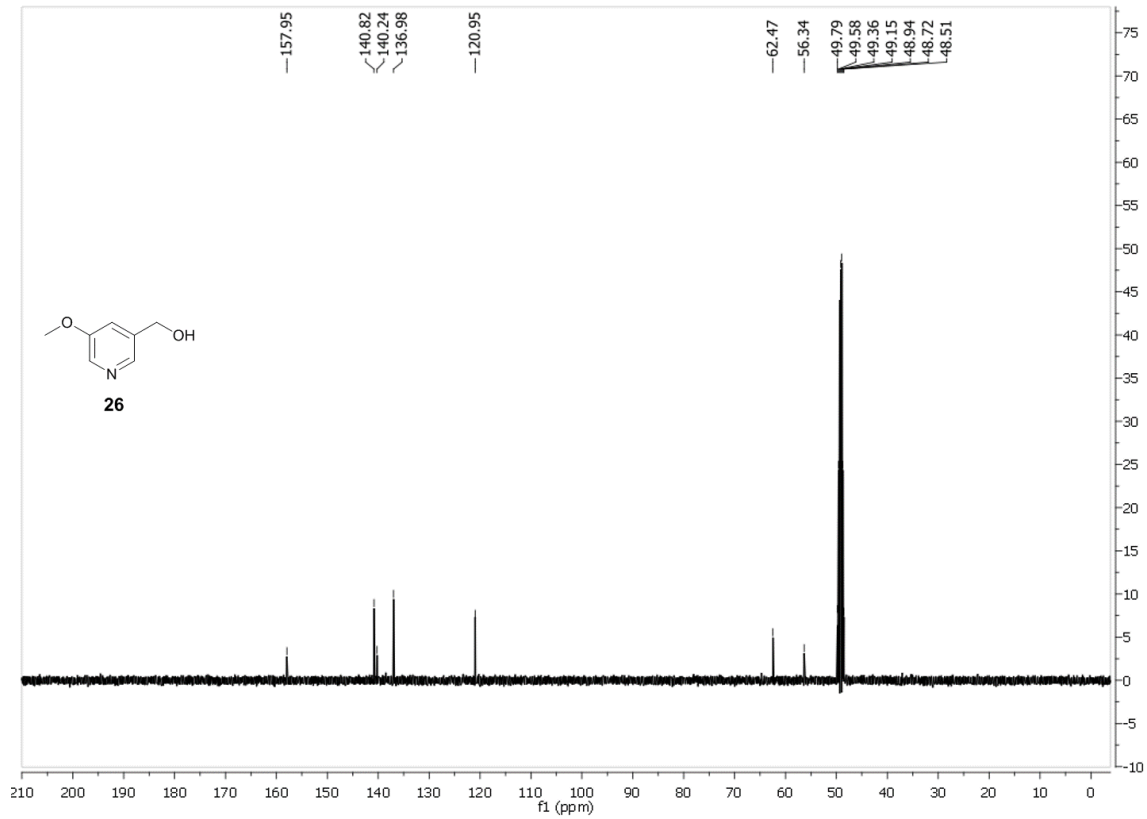
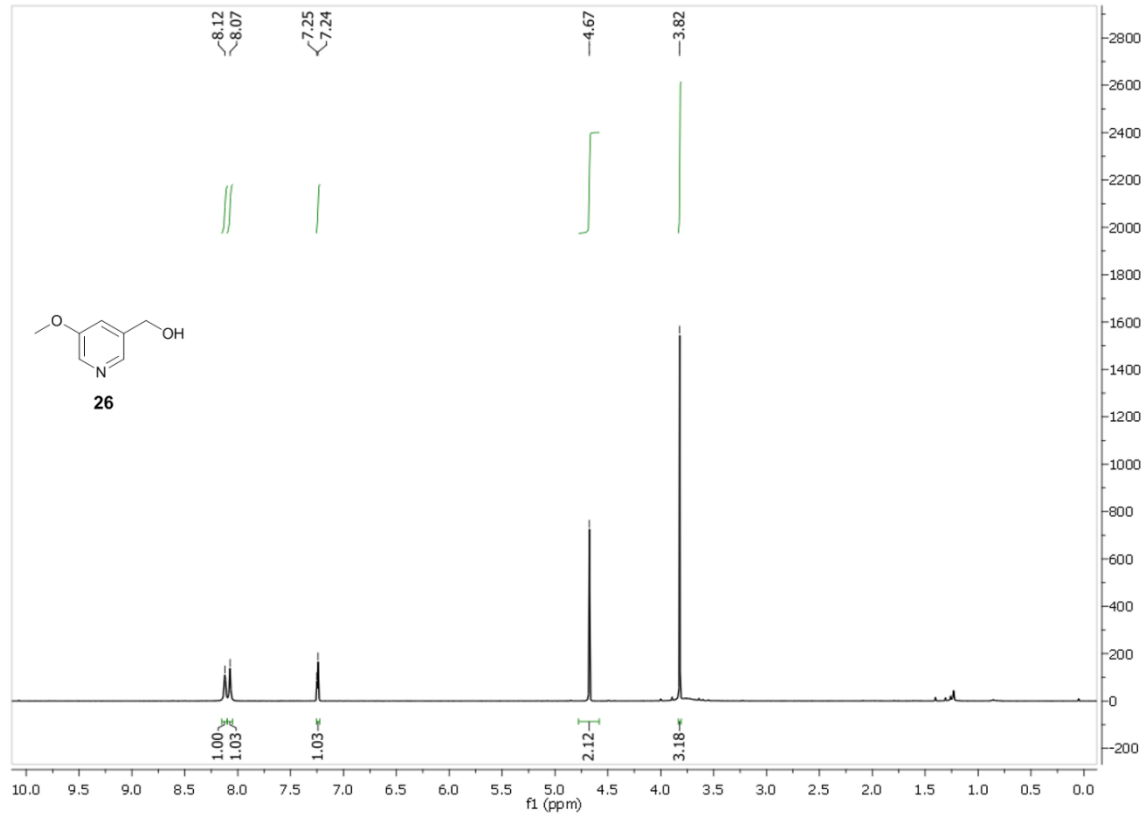


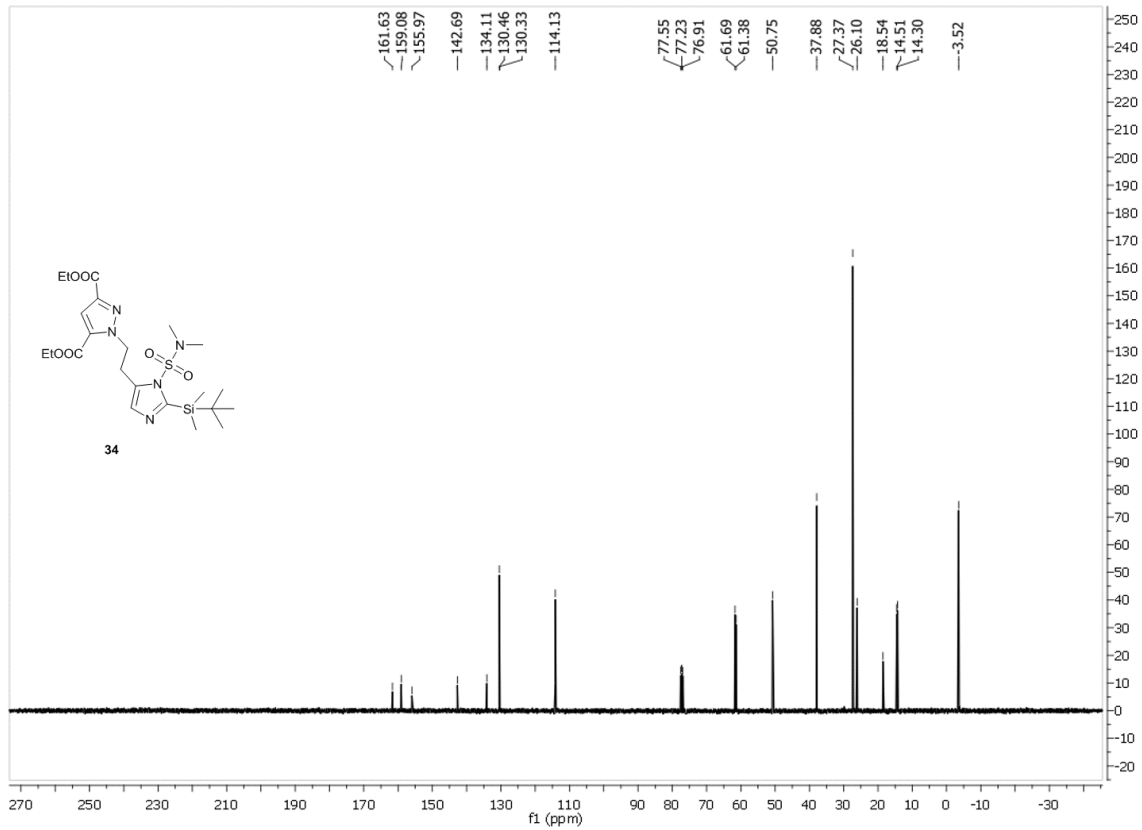
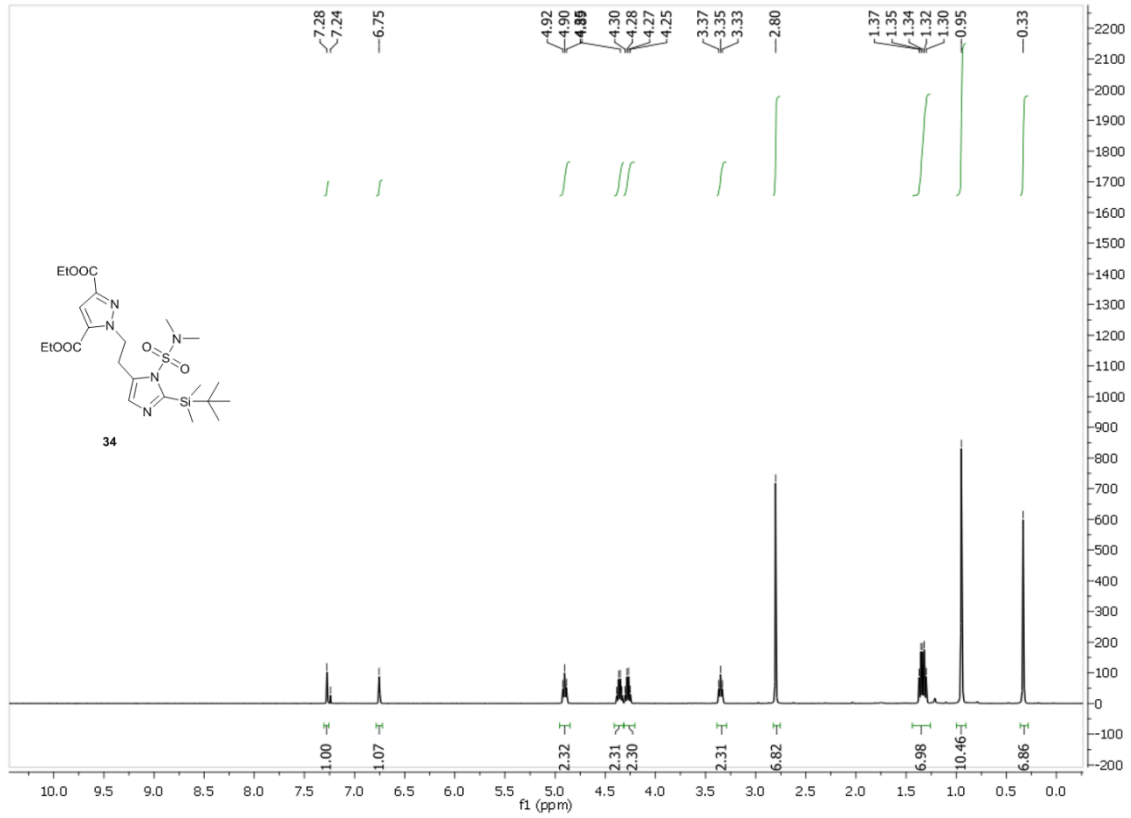


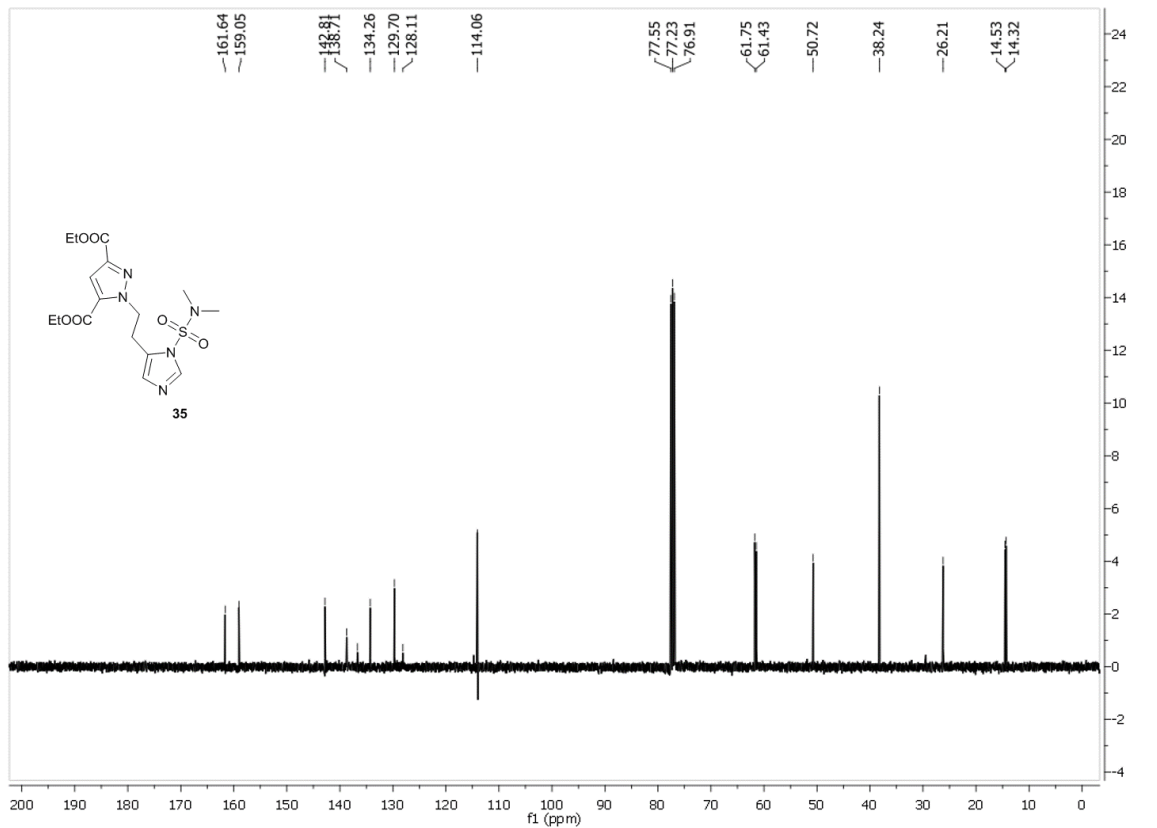
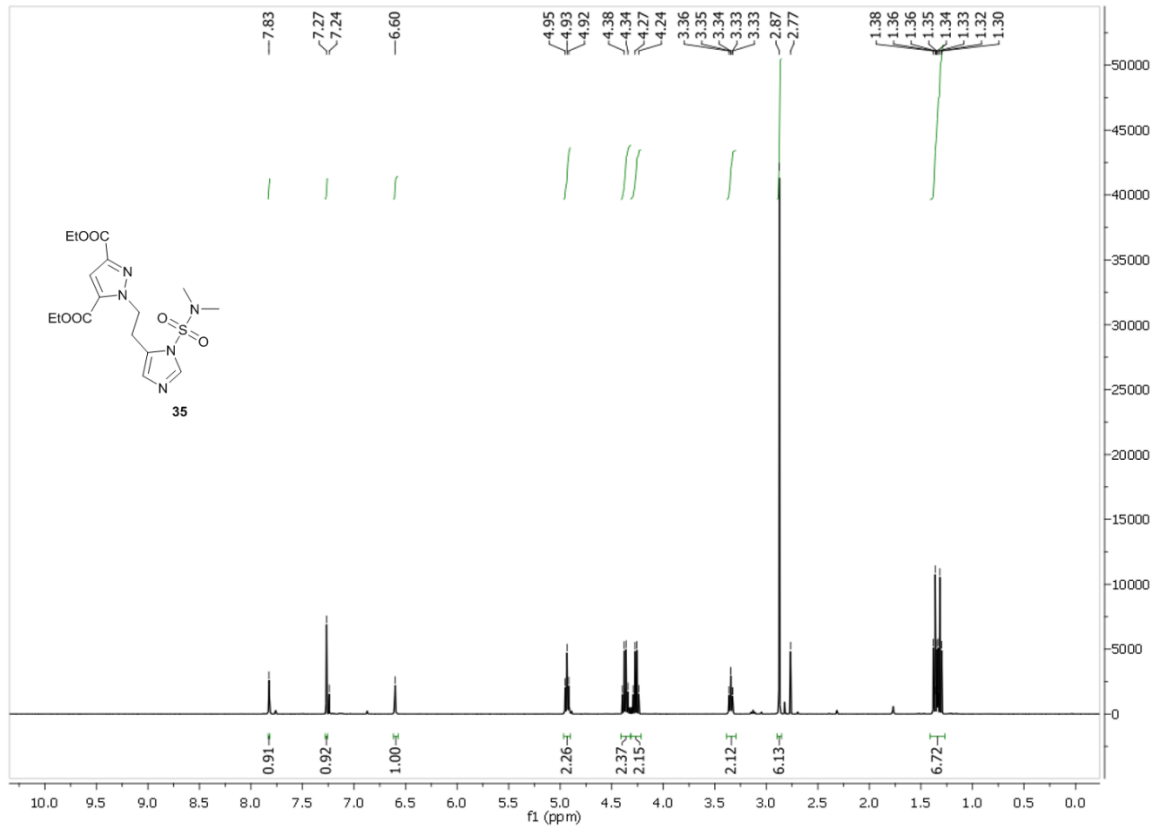


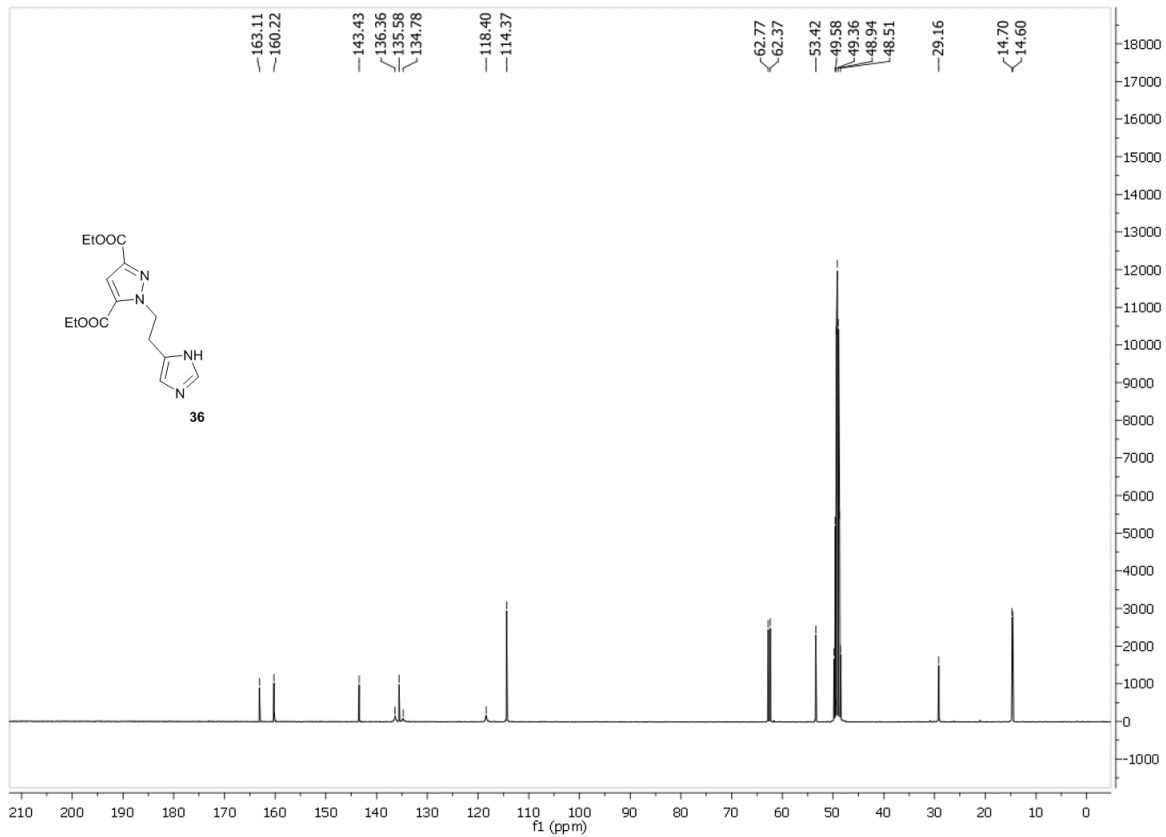
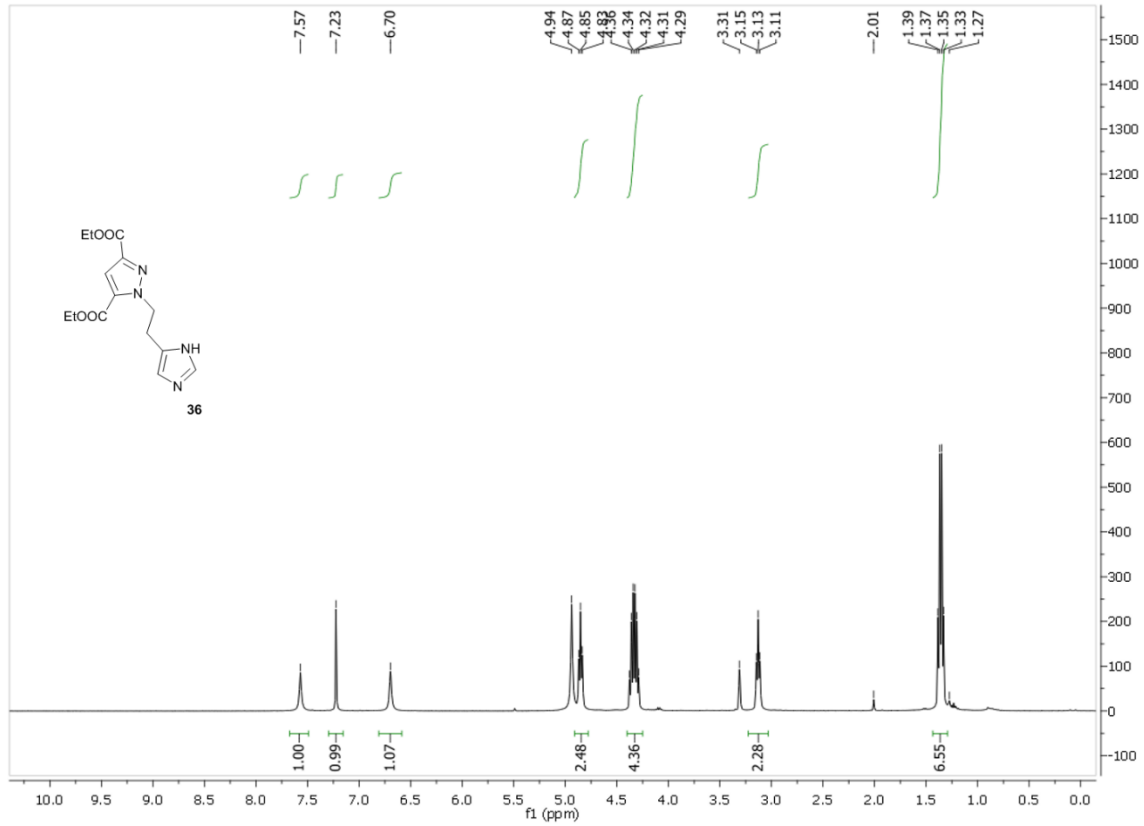


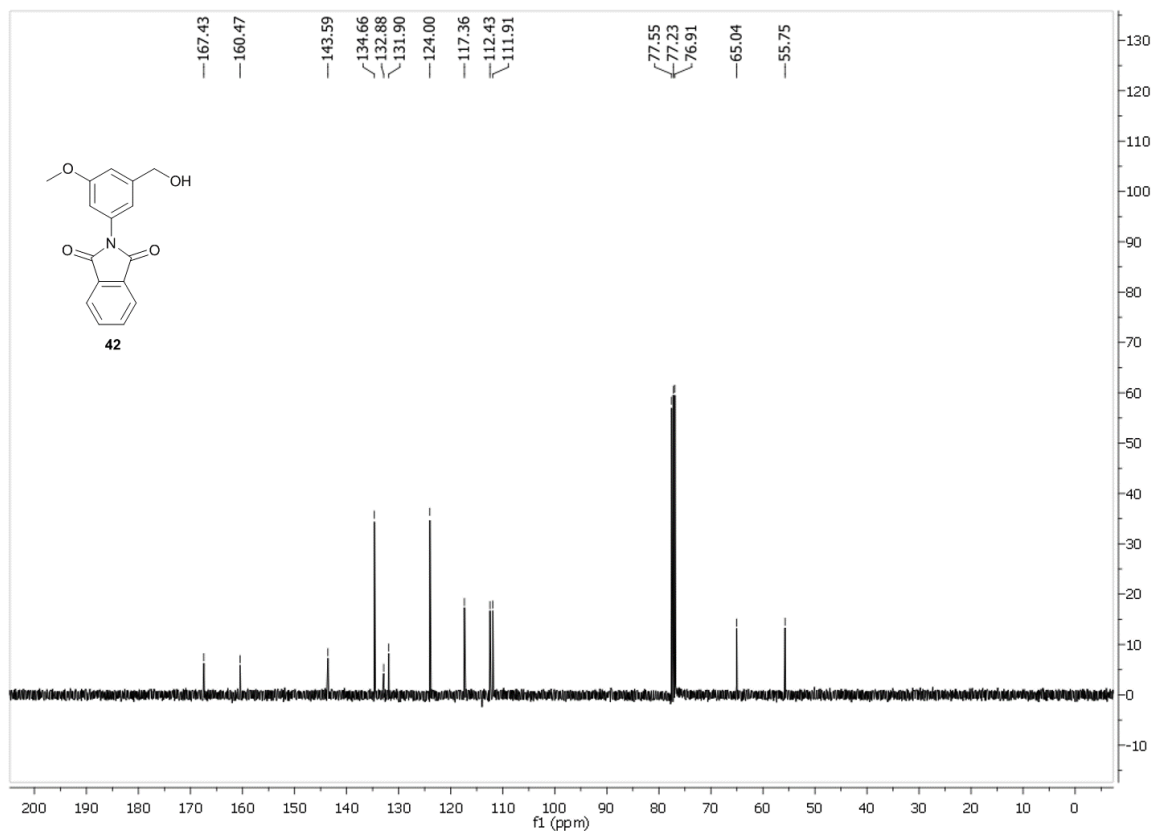
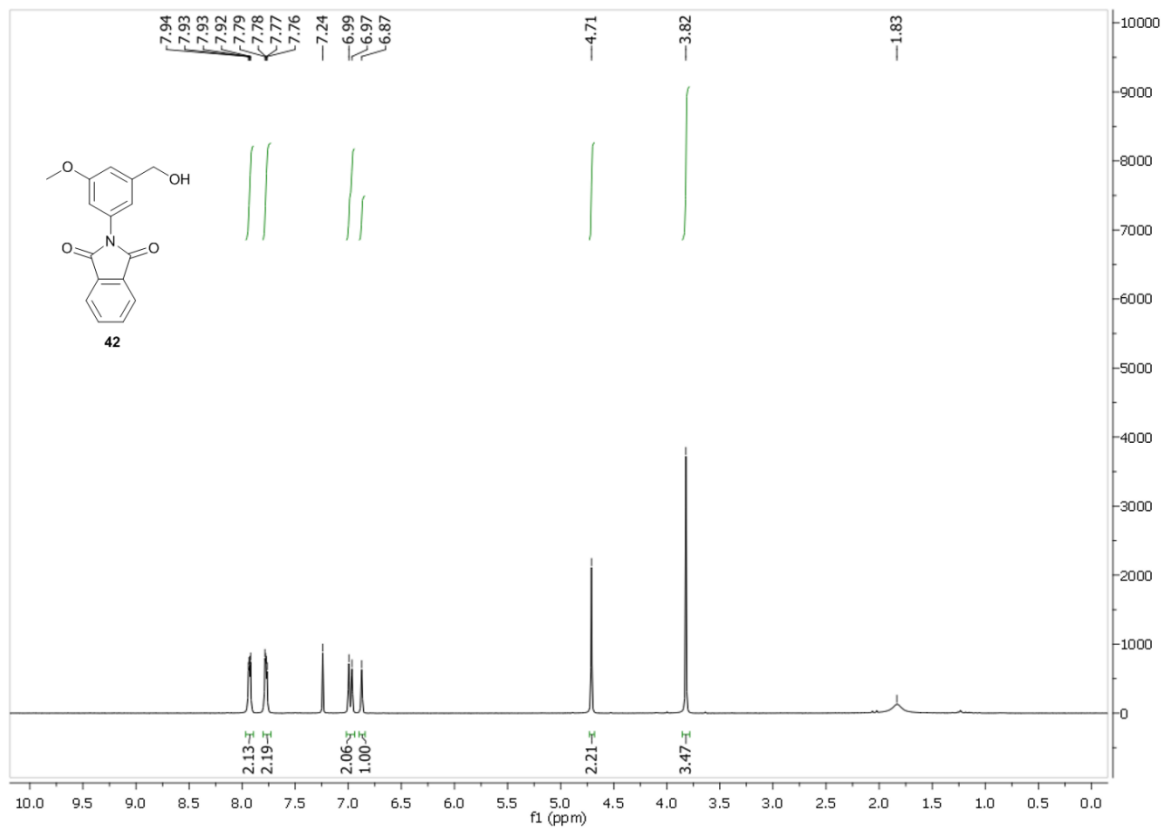


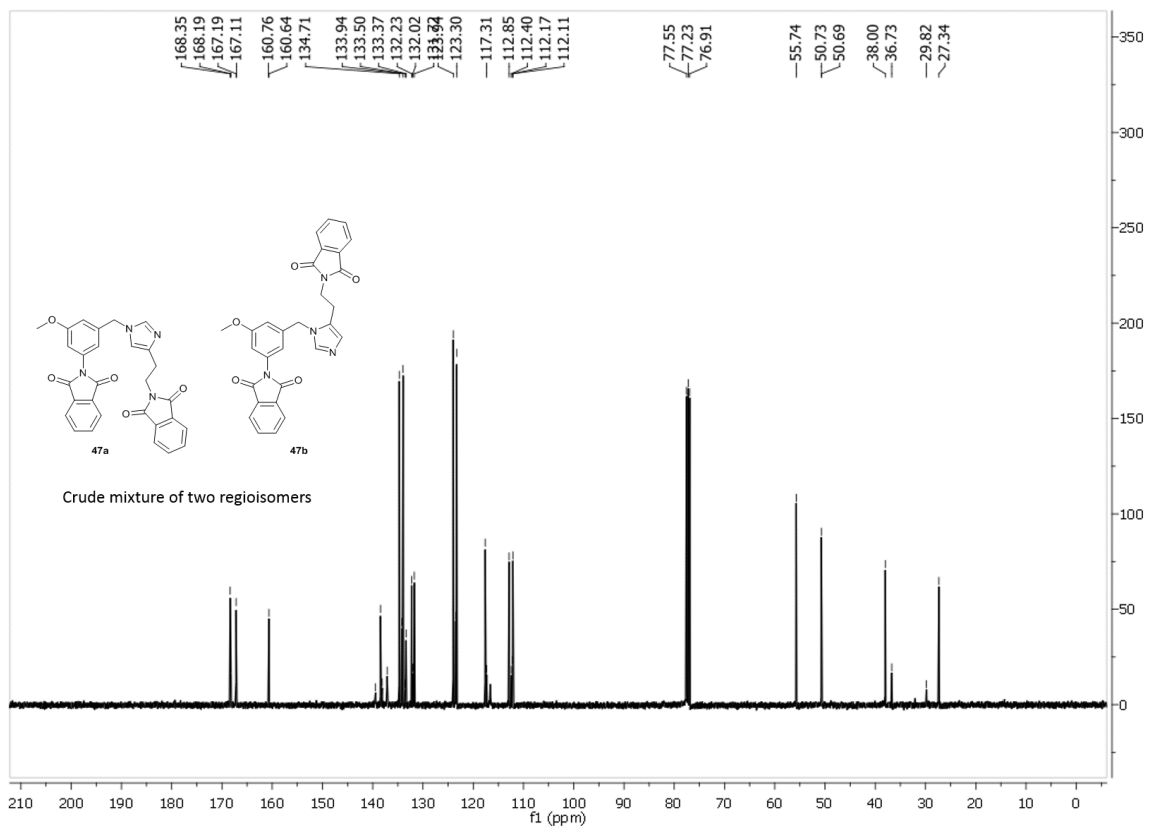
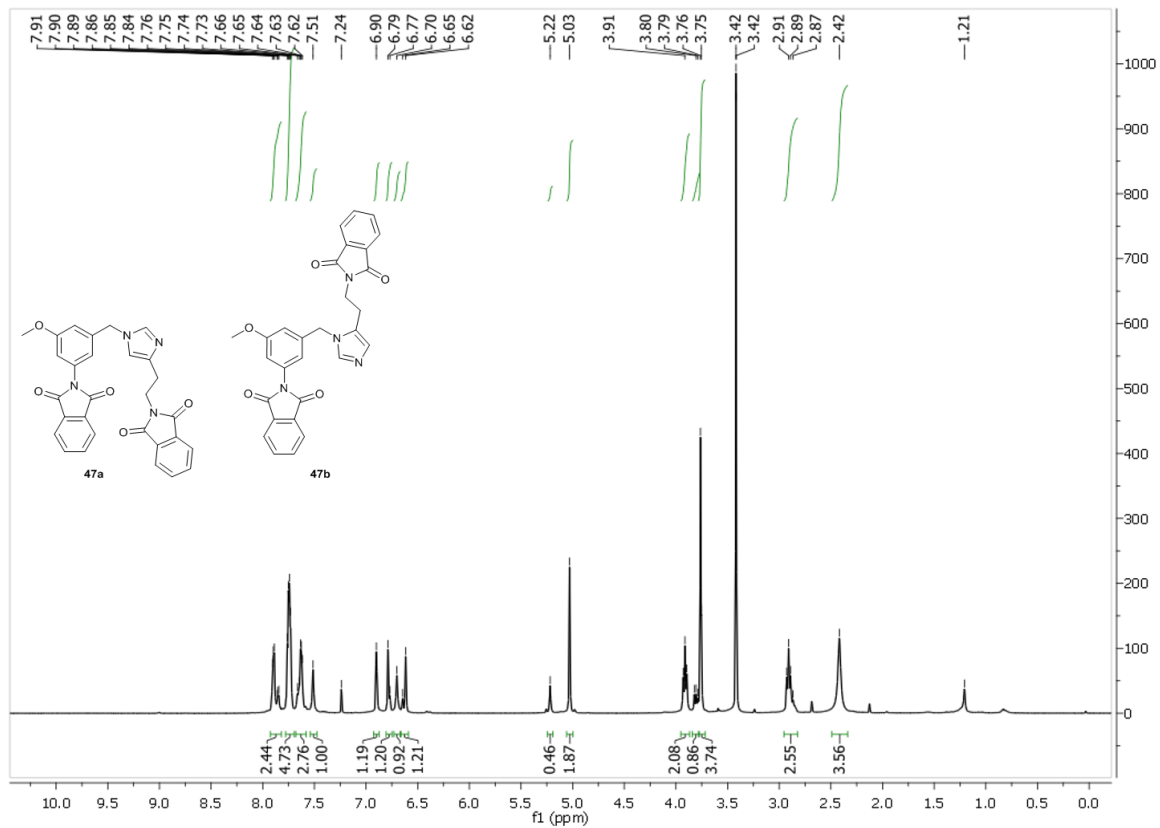














## References

---

- <sup>1</sup> S. Xiang, G. Usunow, G. Lange, M. Busch and L. Tong, *J. Biol. Chem.* 2006, **282**, 2676–2682.
- <sup>2</sup> BioSolveIT GmbH, Sankt Augustin. <http://www.biosolveit.de>, *LeadIT*, 2.1.2.
- <sup>3</sup> a) N. Schneider, S. Hindle, G. Lange, R. Klein, J. Albrecht, H. Briem, K. Beyer, H. Claussen, M. Gastreich, C. Lemmen and M. Rarey, *J. Comput.-Aided Mol. Des.* 2012, **26**, 701–723; b) I. Reulecke, G. Lange, J. Albrecht, R. Klein, M. Rarey, *ChemMedChem* 2008, **3**, 885–897.
- <sup>4</sup> K. Stierand and M. Rarey, *ACS Med. Chem. Lett.* 2010, **1**, 540–545.
- <sup>5</sup> P. R. Gerber and K. Müller, *J. Comput.-Aided Mol. Des.* 1995, **9**, 251–268.
- <sup>6</sup> The PyMOL Molecular Graphics System, Version 1.4. Schrödinger, LLC.
- <sup>7</sup> J. Sadowski, J. Gasteiger and G. Klebe, *J. Chem. Inf. Comput. Sci.* 1994, **34**, 1000–1008.
- <sup>8</sup> G. Neudert and G. Klebe, *Bioinformatics* 2011, **27**, 1021–1022.
- <sup>9</sup> C. Schärfer, T. Shulz-Gash, H.-C. Ehrlich, W. Guba, M. Rarey and M. Stahl, *J. Med. Chem.* 2013, **56**, 2016–2028.
- <sup>10</sup> P. Kuzmic, *Anal. Biochem.* 1996, **237**, 260–273.
- <sup>11</sup> M. Cushman, G. Jin, T. Sambaiah, B. Illarionov, M. Fischer, R. Ladenstein and A. Bacher, *J. Org. Chem.* 2005, **70**, 8162–8170.
- <sup>12</sup> B. Hess, C. Kutzner, D. van der Spoel, E. Lindahl, *J. Chem. Theor. Comp.* 2008, **4**, 435–447.
- <sup>13</sup> V. Hornak, R. Abel, A. Okur, B. Strockbine, A. Roitberg, C. Simmerling, *Proteins* 2006, **65**, 712–725.
- <sup>14</sup> J. Wang, R. M. Wolf, J. W. Caldwell, P. A. Kollman and D. A. Case, *J. Comp. Chem.* 2004, **25**, 1157–1174.
- <sup>15</sup> H. Zhao, L. P. S. de Carvalho, C. Nathan and O. Ouerfelli, *Bioorg. Med. Chem. Lett.* 2010, **20**, 6472–6474.
- <sup>16</sup> M. Wijtmans, S. Celanire, E. Snip, M. R. Gillard, E. Gelens, P. P. Collart, B. J. Venhuis, B. Christophe, S. Hulscher, H. van der Goot, F. Lebon, H. Timmerman, R. A. Bakker, B. I. L. F. Lallemand, R. Leurs, P. E. Talaga and I. J. P. de Esch, *J. Med. Chem.* 2008, **51**, 2944–2953.
- <sup>17</sup> Y. Lee, P. Martasek, L. J. Roman, B. S. S. Masters and R. B. Silverman, *Bioorg. Med. Chem.* 1999, **7**, 1941–1951.

---

<sup>18</sup> C. R. Ganellin, A. Fkyerat, B. Bang-Andersen, S. Athmani, W. Tertiuk, M. Garbarg, X. Ligneau and J.-C. Schwartz, *J. Med. Chem.* 1996, **39**, 3806–3813.

<sup>19</sup> a) S. D. Kuduk, K.-A. Schlegel and Z.-Q. Yang, PCT Int. Appl., 2011084368, 14 Jul 2011; b) H. J. Jung, H.-J. Park, Y.-G. Shin, Y. S. Kim and S.-H. Yoon, *Bull. Korean Chem. Soc.* 2008, **29**, 2277–2280.

<sup>20</sup> Y. Lee, G. Y. Park, H. R. Lucas, P. L. Vajda, K. Kamaraj, M. A. Vance, A. E. Milligan, J. S. Woertink, M. A. Siegler, A. A. Narducci Sarjeant, L. N. Zakharov, A. L. Rheingold, E. I. Solomon and K. D. Karlin. *Inorg. Chem.* 2009, **48**, 11297–11309.

<sup>21</sup> W. J. Thomson and J. Y. Melamed, WO2007/067511A2, 14 June 2007.